Table 1. Association between clinicopathological characteristics of patients and *FHL1* promoter methylation

Characteristics	*FLH1 methylation*		P
	Positive (N = 21)	*Negative (N = 59)*	
Tumor invasion			
⩽T2	13	33	0.80
>T2	8	26	
Lymph node metastasis			
Positive	15	50	0.20
Negative	6	9	
Histological type			
Intestinal	8	27	0.61
Diffuse	13	32	
CIMP			
Positive	17	13	2.9×10^{-6}
Negative	4	46	
EBV infection			
Positive	4	1	0.02
Negative	17	58	
hMLH1 *methylation*			
Positive	4	5	0.23
Negative	17	54	

Abbreviations: CIMP, CGI methylator phenotype; EBV, Epstein–Barr virus.

FHL1 methylation to the formation of an epigenetic field defect, *FHL1* methylation levels were quantified in gastric mucosae of male healthy volunteers (with and without *H. pylori* infection; 16 each) and non-cancerous mucosae of male gastric cancer patients (with and without *H. pylori* infection; 26 each) (Figure 6a). Among the healthy volunteers, *FHL1* methylation was elevated only in *H. pylori*-positive individuals (10 of 16, 62.5%; $P = 0.01$, *t*-test). As potent methylation induction by *H. pylori* can mask a difference in *H. pylori*-positive individuals,[8] *FHL1* methylation levels were compared between healthy volunteers and gastric cancer patients among the *H. pylori*-negative individuals. *FHL1* methylation level was shown to be elevated only in gastric cancer patients (5 of 26, 19.2%; $P = 0.09$, *t*-test). In the case of the colon, *FHL1* methylation was elevated in colonic mucosae of only 2 of 50 colon cancer patients (4%) (Supplementary Figure 5).

FHL1 methylation levels in female specimens

FHL1 methylation levels were analyzed in female specimens, including gastric mucosae of healthy volunteers (18 with *H. pylori* infection and 10 without), those of gastric cancer patients (7 with *H. pylori* infection and 11 without) and one specimen of peripheral leukocytes (Figure 6b). As in male specimens, among the healthy volunteers, *FHL1* methylation levels were significantly elevated in *H. pylori*-positive individuals ($P = 0.01$, *t*-test). Among the *H. pylori*-negative individuals, they tended to be higher in cancer patients than those in healthy volunteers ($P = 0.06$, *t*-test). *FHL1* methylation levels in *H. pylori*-negative female specimens were expected to be 50% because *FHL1* is located on chromosome X, but its actual distribution was between 20 and 40%. Bisulfite sequencing of the *FHL1* promoter region showed that female specimens contained DNA molecules with sparse methylation of CpG sites (Figure 6c), which was in contrast with the dense methylation in cancer specimens (Figure 3b). It was considered that the inactive chromosome X had sparse methylation of the *FHL1* promoter region not detected by qMSP.

DISCUSSION

The *FHL1* gene on chromosome X was shown to be a tumor-suppressor gene in gastrointestinal cancers by the presence of its methylation-silencing, its inhibitory effects on migration, invasion and growth, and the presence of a loss-of-function mutation. Notably, a loss-of-function mutation was identified for the first time in any type of cancers. This added *FHL1* as a new member of 'risky' tumor-suppressor genes on chromosome X, and the first tumor-suppressor gene on chromosome X that can be inactivated by methylation-silencing. *FHL1* methylation was associated with *H. pylori* infection and strongly accumulated in gastric mucosae of gastric cancer patients. Together with the fact that *FHL1* is a tumor-suppressor gene, the accumulation of *FHL1* methylation was considered to contribute to the formation of a field for cancerization as a driver.

Downregulation of *FHL1* in surgical specimens has been reported in breast, renal, prostate,[23] gastric,[25] liver,[21] and lung cancers.[22] The downregulation was associated with short patient survival and deep invasion in gastric cancers,[25] and with poor differentiation in lung cancers.[22] As a mechanism for the downregulation, methylation silencing was described in bladder cancers.[24] Functionally, *FHL1* has been reported to suppress growth of lung, liver and breast cancer cells and transformed fibroblasts,[21,22,26,30] and migration and invasion of bladder cancer cells and transformed fibroblasts.[24,26] The data obtained here were in line with previous reports, and demonstrated that *FHL1* inhibits migration and invasion in gastrointestinal cancer cells.[22]

Mechanistically, FHL1 is characterized by the presence of four and a half highly conserved LIM domains, which are involved in a wide range of protein–protein interactions, including actin cytoskeleton, cellular signaling proteins and transcriptional machinery.[31] In hepatocellular carcinomas, FHL1 was shown to interact with Smad2 and activate TGF-β pathway independently of TGF-β.[21] In breast cancers, FHL1 was shown to interact with estrogen receptor-α and estrogen receptor-β, and repress estrogen-responsive gene transcription.[30] Proteins that interact with FHL1 in gastric and colonic epithelial cells have not been clarified yet. However, inactivation of the TGF-β pathway is known to be involved in these cancers,[32] and is a strong candidate mechanism of how *FHL1* inactivation is involved in these gastrointestinal cancers.

FHL1 methylation was present not only in cancer tissues, but also in non-cancerous gastric mucosae of gastric cancer patients (5 of 26) and in non-cancerous colonic mucosae of colon cancer patients (2 of 50). This showed, for the first time in any types of cancers, that *FHL1* methylation silencing is involved in the formation of the epigenetic field defect as a driver. So far, only a limited number of driver genes, including *CDKN2A*, *CDH1* and *LOX*, are known to be involved in the formation of an epigenetic field defect.[18] For those genes on autosomes, it is difficult to estimate what fraction of cells has biallelic methylation. In contrast, in the case of *FHL1*, its methylation level linearly correlates with the fraction of cells with its inactivation, and, even if its methylation level is low, the presence of its methylation is expected to bring a significant impact. *H. pylori* infection is known to induce aberrant methylation that consists of temporary and permanent components,[8,33] and the high methylation levels in individuals with current *H. pylori* infection were in accordance with this previous finding.

In females, approximately half of the DNA molecules were methylated, densely or sparsely, in gastric mucosae and peripheral leukocytes of healthy volunteers without *H. pylori* infection by bisulfite sequencing. As no methylated DNA molecules were detected in a male specimen, both the densely and sparsely methylated DNA molecules in female specimens were considered to be derived from the inactive X allele.[34] However, we were not able to demonstrate it because a polymorphism that can

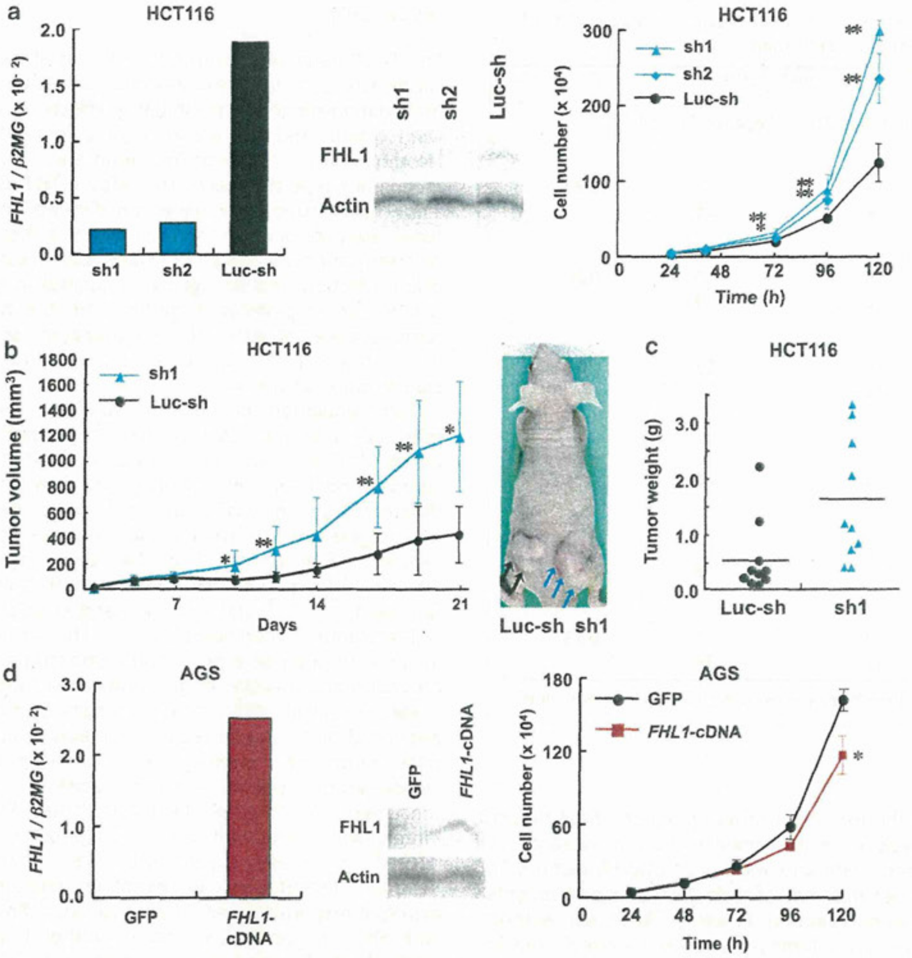

Figure 4. Growth-suppressive activity of *FHL1 in vitro* and *in vivo*. (**a**) *FHL1* knockdown and the resultant increased growth of HCT116 cells. Decreased expression of *FHL1* by its knockdown was confirmed by qRT–PCR (left) and western blot (middle). Growth rates of cells with *FHL1* knockdown were shown to be increased (*$P<0.01$, **$P<0.001$) (right). Data are shown as the mean of three independents ± s.d. (**b**) Increased *in vivo* growth of HCT116 cells with *FHL1* knockdown. Cells with *FHL1* knockdown (sh1) showed a 2.7-fold larger tumor volume compared with the control cells (Luc-sh) (*$P<0.01$, **$P<0.001$). Data are shown as the mean ± s.d. Arrows, tumors produced. (**c**) Increased tumor weight of cells with *FHL1* knockdown (sh1). Mean tumor weight of cells with knockdown (sh1) ($n=10$) was 2.8-fold heavier than that of controls (Luc-sh) ($n=10$). (**d**) Exogenous *FHL1* expression and the resultant decreased growth of AGS cells. Increased levels of *FHL1* expression were confirmed by qRT–PCR (left) and western blot (middle). Growth rates of cells with exogenous *FHL1* were shown to be significantly decreased (*$P<0.01$) (right).

distinguish the allelic origin of mRNA was not present. As qMSP detects only molecules that have dense methylation at primer sites, it was considered that it detected only densely methylated molecules, and methylation levels between 20 and 40% were observed in females.

In conclusion, we showed that *FHL1* on chromosome X is a methylation-silenced tumor-suppressor gene in gastrointestinal cancers, and its methylation in non-cancerous gastric mucosae contributes to the formation of an epigenetic field for cancerization.

MATERIALS AND METHODS

Cell lines and treatment with 5-aza-dC

Sixty-eight cancer cell lines (6 gastric, 7 colon, 12 lung, 12 skin, 7 pancreas, 4 esophageal, 4 prostate, 6 breast and 10 ovary cancer cell lines) and two normal colonic epithelial cells (CRL1790 and CRL1831) were obtained from the American Type Culture Collection (Manassas, VA, USA), Japanese Collection of Research Bioresources (Tokyo, Japan), RIKEN Cell Bank (Tsukuba, Japan) and Tohoku University Cell Resource Center for Biomedical Research (Sendai, Japan)(Supplementary Table 2). HSC39, HSC44 and HSC57 were gifted by Dr K Yanagihara; TMK1 was gifted by Dr W Yasui at Hiroshima University; and GC2 was established by MT For 5-aza-dC treatment. AGS and KATOIII cells were seeded on day 0; media containing freshly prepared 0.3 μM 5-aza-dC were added on days 1 and 3, and cells were harvested on day 5.[35]

Tissue specimens and analysis of *H. pylori* infection status

Cancer specimens were obtained from 80 male gastric cancer patients (average age = 60.4, range = 29–88) and 144 male colon cancer patients (average age = 70, range = 39–98) who underwent gastric and colon resection, respectively, with informed consent. All cancers were histologically diagnosed, and histological types of gastric cancers were classified according to the Lauren classification system (35 intestinal and 45 diffuse type).[36] EBV positivity was determined by *in situ* hybridization targeting *EBER1* using formalin-fixed and paraffin-embedded specimens.[37] The proportion of EBV-positive specimens (5 of 80, 6.3%) was close to EBV prevalence in a previous report (11 of 172, 6.4%).[38]

Normal-appearing gastric mucosae were obtained by endoscopic biopsy of the antral region from 60 healthy volunteers (32 male and 28 female; average age = 52, range = 25–91) and 70 gastric cancer patients

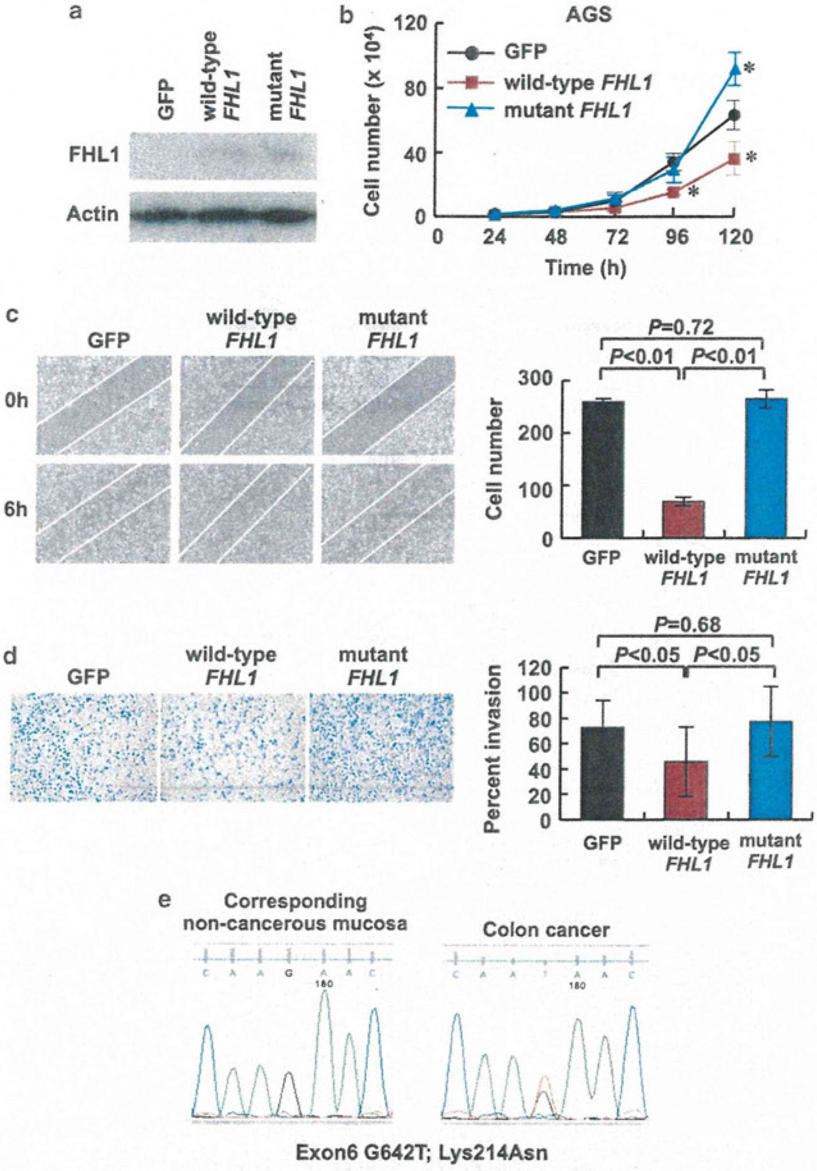

Figure 5. Inhibitory effects of *FHL1* on migration and invasion, and the lack of such functions in *FHL1* with the G642T mutation in AGS. (**a**) Expression levels of exogenous wild-type and mutant *FHL1* detected by western blot. (**b**) The growth-suppressive effect of the wild-type *FHL1*, and the lack of the effect in mutant *FHL1*. Whereas wild-type *FHL1* suppressed cell growth, mutant *FHL1* did not (*$P<0.01$). (**c**) Migration inhibition by wild-type *FHL1*, and the lack of the effect in the mutant *FHL1*. Whereas wild-type *FHL1* inhibited cell migration to 26.6% of the control cells, mutant *FHL1* did not. Photographs were taken at 0 and 6 h after scratching (left), and the number of cells that migrated into the scratched area was counted (mean ± s.d.; right). (**d**) Invasion inhibition by wild-type *FHL1*, and the lack of the effect in the mutant *FHL1*. Whereas wild-type *FHL1* inhibited cell invasion, mutant *FHL1* did not. Representative fields with invading cells on Matrigel-precoated membrane (left). Percent invasion is shown as the mean ± s.d. (right). (**e**) Sequence analysis of colon cancer specimens and corresponding non-cancerous colonic mucosae showed a somatic mutation (G642T; Lys214Asn) in exon 6 of *FHL1*.

(52 male and 18 female; average age = 65, range = 38–85). *H. pylori* infection status was analyzed by a serum anti-*H. pylori* IgG antibody test (SRL, Tokyo, Japan), rapid urease test (Otsuka, Tokushima, Japan) or culture test (Eiken, Tokyo, Japan). Gastric epithelial cells for qRT–PCR analysis were isolated by the gland isolation technique.[39] Normal-appearing colonic mucosae were obtained from a mucosal area distant from colon cancers of surgically resected specimens. Leukocytes were collected from one male (age = 47) and one female (age = 32) volunteer. Specimens were kept frozen at − 80 °C until DNA/RNA extraction. All the analyses using human-derived specimens were approved by the Institutional Review Boards.

Data processing of expression microarray analysis

Expression microarray analysis data in our previous report[19] were used. Signal intensities were scaled so that average signal intensity of all the 18 602 genes would become 500.

Sodium bisulfite modification, MSP, qMSP and bisulfite sequencing

Bisulfite modification was performed using 1 µg of *Bam*HI-digested genomic DNA as previously described.[40] MSP was performed with

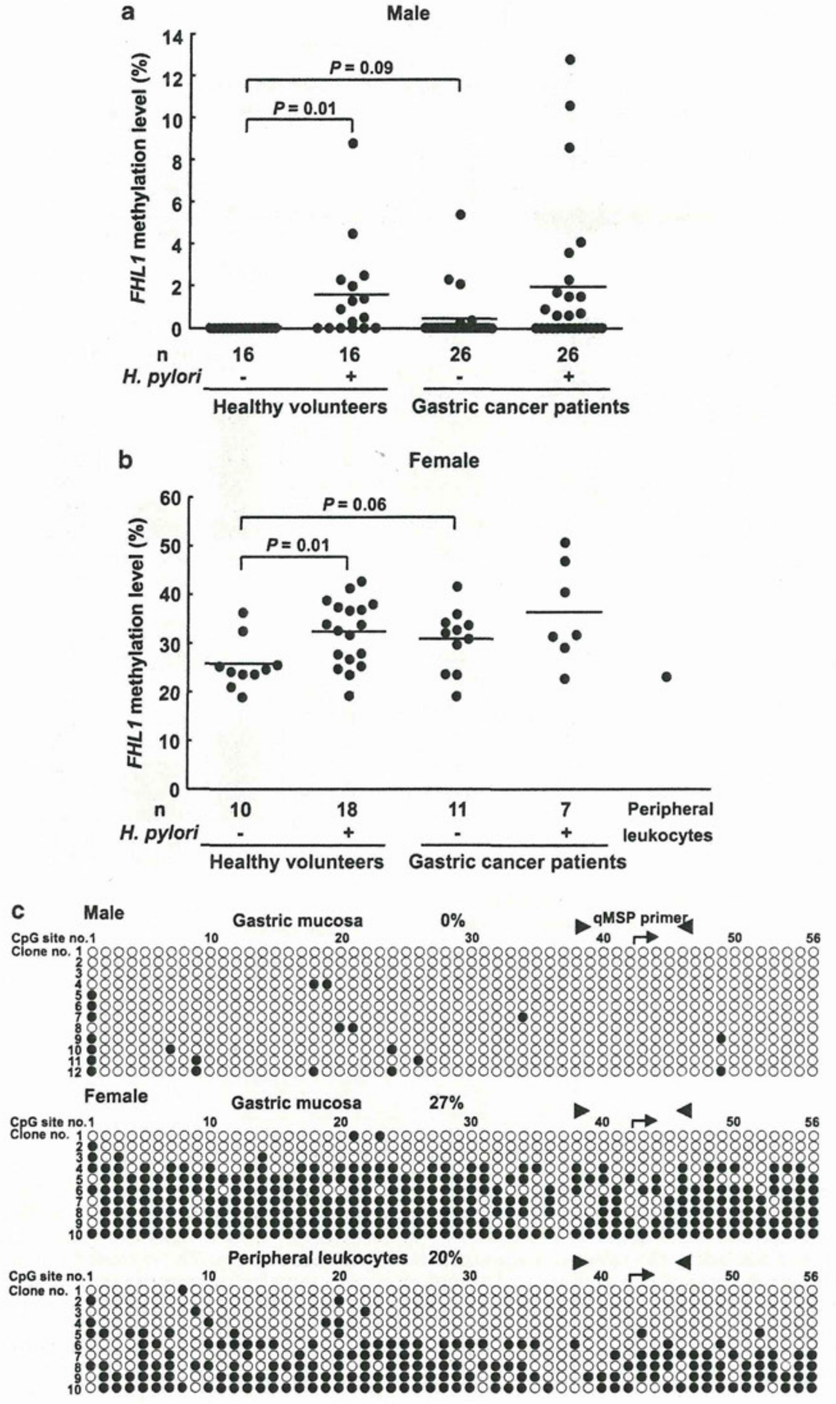

Figure 6. *FHL1* methylation levels in male and female gastric mucosae. (**a**) Methylation levels in male gastric mucosae of healthy volunteers and non-cancerous mucosae of gastric cancer patients. A horizontal line represents the mean methylation level for each group. Among healthy volunteers, *FHL1* methylation was present only in *H. pylori*-positive individuals ($P = 0.01$). Among individuals without *H. pylori* infection, *FHL1* methylation was present only in gastric cancer patients. (**b**) Methylation levels in female gastric mucosae and peripheral leukocytes. *FHL1* methylation levels distributed between 20 and 40%. Methylation levels were higher in *H. pylori*-positive healthy volunteers and gastric cancer patients also in female. (**c**) Bisulfite sequencing of male gastric mucosae, female gastric mucosae and female peripheral leukocytes. Female specimens contained both densely methylated and sparsely methylated DNA molecules, and it was considered that the inactive chromosome X can be densely and sparsely methylated. Closed circle, methylated CpG site; open circle, unmethylated CpG site; arrowheads, primers for qMSP; and arrow, transcription start site.

primer sets specific to methylated and unmethylated sequences (Supplementary Table 3). As controls, fully methylated and unmethylated DNA were prepared by methylating genomic DNA with *SssI* methylase (New England Biolabs, Beverly, MA, USA) and by amplifying genomic DNA with the GenomiPhi amplification system (GE Healthcare, Buckinghamshire, UK), respectively.

Quantitative real-time MSP was performed by real-time PCR using SYBR Green I (BioWhittaker Molecular Applications, Rockland, ME, USA) and an iCycler Thermal Cycler (Bio-Rad Laboratories, Hercules, CA, USA). Although a primer set for MSP was also used for qMSP, a specific annealing temperature in the presence of SYBR Green I was determined (Supplementary Table 3). The number of molecules in a specimen was determined by comparing its amplification with those of standard DNA that contained known numbers of molecules (10^1–10^6 molecules). Based on the numbers of methylated (M) and unmethylated (U) molecules, a methylation level was calculated as the fraction of M molecules in the total number of DNA molecules (no. of M molecules + no. of U molecules). Standard DNA was prepared by cloning PCR products of methylated and unmethylated sequences into a vector (pGEM-T Easy, Promega, Madison, WI, USA). The CIMP status in a gastric cancer was determined as described previously.[27]

Bisulfite sequencing was conducted with primers common to methylated and unmethylated DNA sequences (Supplementary Table 4). The PCR product was cloned into pGEM-T Easy, and 10–12 clones were cycle-sequenced for each specimen.

qRT–PCR

cDNA was synthesized from 1 µg of total RNA using a Superscript III (Invitrogen, Carlsbad, CA, USA). qRT–PCR was performed by real-time PCR using SYBR Green I and an iCycler Thermal Cycler. Standard DNA was prepared by serial dilution of PCR products quantified by the QIAxcel system (QIAGEN, Valencia, CA, USA) after purification using Zymo-Spin I Columns (Zymo Research, Orange, CA, USA).[41] The measured number of cDNA molecules was normalized to that of b2-microglobulin (*b2MG*). The primers and PCR conditions are shown in Supplementary Table 5.

Knockdown and cDNA introduction assays

For a knockdown assay, two pairs and one pair of oligonucleotides were designed against *FHL1* and *Luciferase* (control), respectively (Supplementary Table 6). After annealing of sense and antisense oligonucleotides, the fragment was cloned into a pGreenPuro lentiviral vector (System Biosciences, Mountain View, CA, USA). For cDNA cloning, the entire coding region of human *FHL1* was amplified by RT–PCR (Supplementary Table 7), and cloned into a pCDH-CMV-MCS-EF1-Puro lentiviral vector (System Biosciences). As a control, *copGFP* was cloned into the vector in the same manner. The mutant cDNA was synthesized using the site-directed mutagenesis technique.[42] Using complementary primers carrying mutated sequence (mutation site forward and reverse primers; Supplementary Table 7) and primers for each end of the entire coding region (entire region reverse and forward primers), RT–PCR was performed to generate two DNA fragments that had overlapping ends. These two PCR products were combined by a subsequent PCR with primers for each end of the entire coding region to obtain the mutant cDNA. The mutant cDNA was cloned into a pCDH-CMV-MCS-EF1-Puro lentiviral vector.

The viral vectors and packaging vectors (pPACKH1 HIV Lentivector Packaging Kit, System Biosciences) were cotransfected into 293TN packaging cells, and culture media-containing pseudoviral particles were retrieved. Infection of cancer cell lines with pseudoviral particles was performed according to the manufacturer's protocol (System Biosciences), and stably expressing cells were selected by puromycin without cloning.

Cell growth, migration, invasion and apoptosis analysis

Cell growth was analyzed by seeding cells in triplicate in a six-well plate (3×10^4 cells, AGS; 1×10^5 cells, HSC39) and in a 12-well plate (5×10^3 cells, HCT116). Their numbers were counted at 24, 48, 72, 96 and 120 h. Three independent cultures were performed for one experiment.

Cell migration was analyzed by a wound-healing assay.[43] Cells were seeded in triplicate in a 6-cm dish coated with type I collagen (1×10^6 cells, AGS; 4×10^6 cells, MKN28), and cultured in RPMI-1640 medium containing 1% fetal calf serum to form a monolayer. The cell monolayer was scraped in a straight line with a pipette tip. After incubation for 6 and 12 h, the migrating cells were observed under bright-field microscopy. Three independent cultures were performed for one experiment.

Cell invasion was analyzed by a Matrigel invasion assay, using a Boyden chamber with the Matrigel-precoated membrane or Matrigel-free membrane in the top chamber (BD Biosciences, Bedford, MA, USA). Cells were seeded in top chambers in serum-free RPMI1640 (5×10^4 cells, AGS; 1×10^5 cells, MKN28), and the bottom chambers were filled with RPMI1640 containing 10% fetal calf serum. After incubation for 24 and 48 h (AGS and MKN28, respectively), the area of cells invading through the top chambers was measured by ImageJ software (version 1.38, National Institutes of Health, Bethesda, MD, USA). Percent invasion was calculated as the area of cells invading through the Matrigel-precoated membrane relative to those through Matrigel-free membrane. Three independent cultures were performed for one experiment and the experiment was repeated three times.

The apoptosis of the cells was analyzed by terminal deoxynucleotidyl transferase dUTP nick end labeling assay, using an *in situ* cell death detection kit, TMRred (Roche, Basel, Switzerland).

Tumor formation assay in nude mice

Cells (8×10^6 cells, HCT116) were inoculated subcutaneously on both flanks of 7-week-old male athymic nude mice (BALB/cAJc1-nu/nu; CLEA, Tokyo, Japan). Tumor sizes were measured with calipers every 3 days and the volume was calculated as (length $\times$ width^2) $\times$ 0.5, and tumor weights were measured at their killing on day 22. All the animal experiments were approved by the Animal Experiment Ethical Committee at the National Cancer Center.

Mutation analysis

All seven exons of *FHL1* were amplified using 100 ng of genomic DNA with primers located in introns, except for one primer on exon 7 (Supplementary Table 8). The PCR products were directly cycle-sequenced with a BigDye Terminator kit (PE Biosystems, Foster City, CA, USA) and an ABI PRISM 310 automated DNA sequencer (PE Biosystems).

Statistical analysis

Differences in mean methylation levels, expression levels, cell numbers and tumor sizes were analyzed by the Welch *t*-test. Association between *FHL1* methylation and clinicopathological factors was analyzed by the χ^2 test. All the analyses were performed using SPSS (SPSS, Inc., Chicago, IL, USA), and the results were considered significant when a P value < 0.05 was obtained by two-sided tests.

CONFLICT OF INTEREST

The authors declare no conflict of interest.

ACKNOWLEDGEMENTS

We thank Dr Yanagihara and Dr Yasui for their kind gift of cell lines. This study was supported by a Grant-in-Aid for the Third-term Comprehensive Cancer Control Strategy from the Ministry of Health, Labour and Welfare, Japan, and by the National Cancer Center Research and Development Fund. TA is a recipient of the Research Resident Fellowship from the Foundation for Promotion of Cancer Research.

REFERENCES

1 Knudson AG. Two genetic hits (more or less) to cancer. *Nat Rev Cancer* 2001; **1**: 157–162.
2 Ushijima T. Detection and interpretation of altered methylation patterns in cancer cells. *Nat Rev Cancer* 2005; **5**: 223–231.
3 Jones PA, Baylin SB. The epigenomics of cancer. *Cell* 2007; **128**: 683–692.
4 Rivera MN, Kim WJ, Wells J, Driscoll DR, Brannigan BW, Han M *et al.* An X chromosome gene, WTX, is commonly inactivated in Wilms tumor. *Science* 2007; **315**: 642–645.
5 Zuo T, Wang L, Morrison C, Chang X, Zhang H, Li W *et al.* FOXP3 is an X-linked breast cancer suppressor gene and an important repressor of the HER-2/ErbB2 oncogene. *Cell* 2007; **129**: 1275–1286.
6 Wang L, Liu R, Li W, Chen C, Katoh H, Chen GY *et al.* Somatic single hits inactivate the X-linked tumor suppressor FOXP3 in the prostate. *Cancer Cell* 2009; **16**: 336–346.
7 Van Vlierberghe P, Palomero T, Khiabanian H, Van Der Meulen J, Castillo M, Van Roy N *et al.* PHF6 mutations in T-cell acute lymphoblastic leukemia. *Nat Genet* 2010; **42**: 338–342.

8 Maekita T, Nakazawa K, Mihara M, Nakajima T, Yanaoka K, Iguchi M *et al.* High levels of aberrant DNA methylation in Helicobacter pylori-infected gastric mucosae and its possible association with gastric cancer risk. *Clin Cancer Res* 2006; **12**: 989–995.

9 Ando T, Yoshida T, Enomoto S, Asada K, Tatematsu M, Ichinose M *et al.* DNA methylation of microRNA genes in gastric mucosae of gastric cancer patients: its possible involvement in the formation of epigenetic field defect. *Int J Cancer* 2009; **124**: 2367–2374.

10 Shen L, Kondo Y, Rosner GL, Xiao L, Hernandez NS, Vilaythong J *et al.* MGMT promoter methylation and field defect in sporadic colorectal cancer. *J Natl Cancer Inst* 2005; **97**: 1330–1338.

11 Kondo Y, Kanai Y, Sakamoto M, Mizokami M, Ueda R, Hirohashi S. Genetic instability and aberrant DNA methylation in chronic hepatitis and cirrhosis—a comprehensive study of loss of heterozygosity and microsatellite instability at 39 loci and DNA hypermethylation on 8 CpG islands in microdissected specimens from patients with hepatocellular carcinoma. *Hepatology* 2000; **32**: 970–979.

12 Ishii T, Murakami J, Notohara K, Cullings HM, Sasamoto H, Kambara T *et al.* Oesophageal squamous cell carcinoma may develop within a background of accumulating DNA methylation in normal and dysplastic mucosa. *Gut* 2007; **56**: 13–19.

13 Oka D, Yamashita S, Tomioka T, Nakanishi Y, Kato H, Kaminishi M *et al.* The presence of aberrant DNA methylation in noncancerous esophageal mucosae in association with smoking history: a target for risk diagnosis and prevention of esophageal cancers. *Cancer* 2009; **115**: 3412–3426.

14 Lee YC, Wang HP, Wang CP, Ko JY, Lee JM, Chiu HM *et al.* Revisit of field cancerization in squamous cell carcinoma of upper aerodigestive tract: better risk assessment with epigenetic markers. *Cancer Prev Res* 2011; **4**: 1982–1992.

15 Yan PS, Venkataramu C, Ibrahim A, Liu JC, Shen RZ, Diaz NM *et al.* Mapping geographic zones of cancer risk with epigenetic biomarkers in normal breast tissue. *Clin Cancer Res* 2006; **12**: 6626–6636.

16 Arai E, Kanai Y, Ushijima S, Fujimoto H, Mukai K, Hirohashi S. Regional DNA hypermethylation and DNA methyltransferase (DNMT) 1 protein overexpression in both renal tumors and corresponding nontumorous renal tissues. *Int J Cancer* 2006; **119**: 288–296.

17 Nakajima T, Maekita T, Oda I, Gotoda T, Yamamoto S, Umemura S *et al.* Higher methylation levels in gastric mucosae significantly correlate with higher risk of gastric cancers. *Cancer Epidemiol Biomarkers Prev* 2006; **15**: 2317–2321.

18 Ushijima T. Epigenetic field for cancerization. *J Biochem Mol Biol* 2007; **40**: 142–150.

19 Yamashita S, Tsujino Y, Moriguchi K, Tatematsu M, Ushijima T. Chemical genomic screening for methylation-silenced genes in gastric cancer cell lines using 5-aza-2′-deoxycytidine treatment and oligonucleotide microarray. *Cancer Sci* 2006; **97**: 64–71.

20 Ushijima T, Watanabe N, Shimizu K, Miyamoto K, Sugimura T, Kaneda A. Decreased fidelity in replicating CpG methylation patterns in cancer cells. *Cancer Res* 2005; **65**: 11–17.

21 Ding L, Wang Z, Yan J, Yang X, Liu A, Qiu W *et al.* Human four-and-a-half LIM family members suppress tumor cell growth through a TGF-beta-like signaling pathway. *J Clin Invest* 2009; **119**: 349–361.

22 Niu C, Liang C, Guo J, Cheng L, Zhang H, Qin X *et al.* Downregulation and growth inhibitory role of FHL1 in lung cancer. *Int J Cancer* 2012; **130**: 2549–2556.

23 Li X, Jia Z, Shen Y, Ichikawa H, Jarvik J, Nagele RG *et al.* Coordinate suppression of Sdpr and Fhl1 expression in tumors of the breast, kidney, and prostate. *Cancer Sci* 2008; **99**: 1326–1333.

24 Matsumoto M, Kawakami K, Enokida H, Toki K, Matsuda R, Chiyomaru T *et al.* CpG hypermethylation of human four-and-a-half LIM domains 1 contributes to migration and invasion activity of human bladder cancer. *Int J Mol Med* 2010; **26**: 241–247.

25 Sakashita K, Mimori K, Tanaka F, Kamohara Y, Inoue H, Sawada T *et al.* Clinical significance of loss of Fhl1 expression in human gastric cancer. *Ann Surg Oncol* 2008; **15**: 2293–2300.

26 Shen Y, Jia Z, Nagele RG, Ichikawa H, Goldberg GS. SRC uses Cas to suppress Fhl1 in order to promote nonanchored growth and migration of tumor cells. *Cancer Res* 2006; **66**: 1543–1552.

27 Enomoto S, Maekita T, Tsukamoto T, Nakajima T, Nakazawa K, Tatematsu M *et al.* Lack of association between CpG island methylator phenotype in human gastric cancers and methylation in their background non-cancerous gastric mucosae. *Cancer Sci* 2007; **98**: 1853–1861.

28 Ota N, Kawakami K, Okuda T, Takehara A, Hiranuma C, Oyama K *et al.* Prognostic significance of p16(INK4a) hypermethylation in non-small cell lung cancer is evident by quantitative DNA methylation analysis. *Anticancer Res* 2006; **26**: 3729–3732.

29 Matsusaka K, Kaneda A, Nagae G, Ushiku T, Kikuchi Y, Hino R *et al.* Classification of Epstein-Barr virus-positive gastric cancers by definition of DNA methylation epigenotypes. *Cancer Res* 2011; **71**: 7187–7197.

30 Ding L, Niu C, Zheng Y, Xiong Z, Liu Y, Lin J *et al.* FHL1 interacts with oestrogen receptors and regulates breast cancer cell growth. *J Cell Mol Med* 2011; **15**: 72–85.

31 Shathasivam T, Kislinger T, Gramolini AO. Genes proteins and complexes: the multifaceted nature of FHL family proteins in diverse tissues. *J Cell Mol Med* 2010; **14**: 2702–2720.

32 Achyut BR, Yang L. Transforming growth factor-beta in the gastrointestinal and hepatic tumor microenvironment. *Gastroenterol* 2011; **141**: 1167–1178.

33 Niwa T, Tsukamoto T, Toyoda T, Mori A, Tanaka H, Maekita T *et al.* Inflammatory Processes Triggered by Helicobacter pylori Infection Cause Aberrant DNA Methylation in Gastric Epithelial Cells. *Cancer Res* 2010; **70**: 1430–1440.

34 Panning B, Jaenisch R. RNA and the epigenetic regulation of X chromosome inactivation. *Cell* 1998; **93**: 305–308.

35 Moriguchi K, Yamashita S, Tsujino Y, Tatematsu M, Ushijima T. Larger numbers of silenced genes in cancer cell lines with increased de novo methylation of scattered CpG sites. *Cancer Lett* 2007; **249**: 178–187.

36 Lauren P. The two histological main types of gastric carcinoma: diffuse and so-called intestinal-type carcinoma. An attempt at a histo-clinical classification. *Acta Pathol Microbiol Scand* 1965; **64**: 31–49.

37 Fukayama M, Hayashi Y, Iwasaki Y, Chong J, Ooba T, Takizawa T *et al.* Epstein-Barr virus-associated gastric carcinoma and Epstein-Barr virus infection of the stomach. *Lab Invest* 1994; **71**: 73–81.

38 Luo B, Wang Y, Wang XF, Liang H, Yan LP, Huang BH *et al.* Expression of Epstein-Barr virus genes in EBV-associated gastric carcinomas. *World J Gastroenterol* 2005; **11**: 629–633.

39 Cheng H, Bjerknes M, Amar J. Methods for the determination of epithelial cell kinetic parameters of human colonic epithelium isolated from surgical and biopsy specimens. *Gastroenterol* 1984; **86**: 78–85.

40 Kaneda A, Kaminishi M, Sugimura T, Ushijima T. Decreased expression of the seven ARP2/3 complex genes in human gastric cancers. *Cancer Lett* 2004; **212**: 203–210.

41 Hosoya K, Yamashita S, Ando T, Nakajima T, Itoh F, Ushijima T. Adenomatous polyposis coli 1A is likely to be methylated as a passenger in human gastric carcinogenesis. *Cancer Lett* 2009; **285**: 182–189.

42 Ho SN, Hunt HD, Horton RM, Pullen JK, Pease LR. Site-directed mutagenesis by overlap extension using the polymerase chain reaction. *Gene* 1989; **77**: 51–59.

43 Liang CC, Park AY, Guan JL. *In vitro* scratch assay: a convenient and inexpensive method for analysis of cell migration *in vitro*. *Nat Protoc* 2007; **2**: 329–333.

Supplementary Information accompanies the paper on the Oncogene website (http://www.nature.com/onc)

Cancer Letters 330 (2013) 33–40

Contents lists available at SciVerse ScienceDirect

Cancer Letters

journal homepage: www.elsevier.com/locate/canlet

Comprehensive DNA methylation and extensive mutation analyses reveal an association between the CpG island methylator phenotype and oncogenic mutations in gastric cancers

Jeong Goo Kim [a,b], Hideyuki Takeshima [a], Tohru Niwa [a], Emil Rehnberg [a], Yasuyuki Shigematsu [a], Yukie Yoda [a,c], Satoshi Yamashita [a], Ryoji Kushima [d], Takao Maekita [e], Masao Ichinose [e], Hitoshi Katai [c], Won Sang Park [f], Young Seon Hong [g], Cho Hyun Park [b,*], Toshikazu Ushijima [a,*]

[a] Division of Epigenomics, National Cancer Center Research Institute, 5-1-1 Tsukiji, Chuo-ku, Tokyo 104-0045, Japan
[b] Department of Surgery, College of Medicine, The Catholic University of Korea, 222 Banpo-daero, Seocho-gu, Seoul 137-701, Republic of Korea
[c] Gastric Surgery Division, National Cancer Center Hospital, 5-1-1 Tsukiji, Chuo-ku, Tokyo 104-0045, Japan
[d] Pathology Division and Clinical Laboratory, National Cancer Center Hospital, 5-1-1 Tsukiji, Chuo-ku, Tokyo 104-0045, Japan
[e] Second Department of Internal Medicine, Wakayama Medical University, 811-1, Kimiidera, Wakayama 641-8509, Japan
[f] Department of Pathology, College of Medicine, The Catholic University of Korea, 222 Banpo-daero, Seocho-gu, Seoul 137-701, Republic of Korea
[g] Department of Internal Medicine, College of Medicine, The Catholic University of Korea, 222 Banpo-daero, Seocho-gu, Seoul 137-701, Republic of Korea

ARTICLE INFO

Article history:
Received 10 October 2012
Received in revised form 12 November 2012
Accepted 12 November 2012

Keywords:
Epigenetics
Aberrant DNA methylation
CIMP
Mutation
Gastric cancer

ABSTRACT

Recent development of personal sequencers for extensive mutation analysis and bead array technology for comprehensive DNA methylation analysis have made it possible to obtain integrated pictures of genetic and epigenetic alterations on the same set of cancer samples. Here, we aimed to establish such pictures of gastric cancers (GCs). Comprehensive methylation analysis of 30 GCs revealed that the number of aberrantly methylated genes was highly variable among individual GCs. Extensive mutation analysis of 55 known cancer-related genes revealed that 19 of the 30 GCs had 24 somatic mutations of eight different genes (*CDH1*, *CTNNB1*, *ERBB2*, *KRAS*, *MLH1*, *PIK3CA*, *SMARCB1*, and *TP53*). Integration of information on the genetic and epigenetic alterations revealed that the GCs with the CpG island methylator phenotype (CIMP) tended to have mutations of oncogenes, *CTNNB1*, *ERBB2*, *KRAS*, and *PIK3CA*. This is one of the first studies in which both genetic and epigenetic alterations were extensively analyzed in the same set of samples. It was also demonstrated for the first time in GCs that the CIMP was associated with oncogene mutations.

1. Introduction

Both genetic and epigenetic alterations are important for human carcinogenesis [1,2]. Genetic alterations are responsible for activation of oncogenes and inactivation of tumor-suppressor genes [2]. In human gastric cancers (GCs), oncogenes activated by mutations include *CTNNB1* (β-catenin), *ERBB2*, and *PIK3CA* [3–10], and tumor-suppressor genes inactivated by mutations include *CDH1* (E-cadherin), *CDKN2A* (*p16*), *TP53*, and *ARID1A* [11,12]. Even by whole exome sequencing of GCs, the vast majority of driver genes identified were known cancer-related genes, and novel genes identified, such as *ARID1A* and *FAT4*, had only low incidences of mutations [11,12]. This indicates that extensive mutation analysis of a large number of known cancer-related genes can provide an overall picture of a cancer sample, and this is now possible with high speed and low cost by using next-generation personal sequencers [13,14].

Epigenetic alterations, namely aberrant DNA methylation of promoter CpG islands (CGIs), are also responsible for inactivation of various tumor-suppressor genes [1]. DNA methylation statuses of the entire genome can be now comprehensively analyzed using microarray technologies, and bead array technology is especially useful for its quantitative measurement [15]. In GCs, tumor-suppressor genes inactivated by promoter methylation include *CDH1*, *CDKN2A*, *FHL1*, *LOX*, *MLH1*, and *SFRP* family genes (*SFRP1*, *SFRP2*, and *SFRP5*) [16–21]. These tumor-suppressor genes are more frequently inactivated by aberrant methylation than by genetic alterations in GCs [22]. In addition, aberrant methylation is induced in gastric mucosae by *Helicobacter pylori* (*H. pylori*)

Abbreviations: GC, gastric cancer; CGI, CpG island; *H. pylori*, *Helicobacter pylori*; CIMP, CpG island methylator phenotype; EB virus, Epstein–Barr virus; TSS, transcription start site; COSMIC, Catalogue Of Somatic Mutations In Cancer.

* Corresponding authors. Fax: +81 3 5565 1753.
E-mail address: tushijim@ncc.go.jp (T. Ushijima).

0304-3835/$ - see front matter © 2012 Elsevier Ireland Ltd. All rights reserved.
http://dx.doi.org/10.1016/j.canlet.2012.11.022

infection [23,24], a well-established major inducer of human GCs [25]. The frequent inactivation of tumor-suppressor genes by aberrant methylation and the deep involvement of *H. pylori* infection in its induction indicate the importance of epigenetic alterations in GCs.

Not only in GCs but also in other types of cancers, a subgroup of cancers is known to have frequent aberrant DNA methylation of CGIs, referred to as the CpG island methylator phenotype (CIMP). The CIMP was first described in colorectal cancers [26], and is associated with unique clinicopathological features. For example, the CIMP is associated with poor prognosis in colorectal cancers, lung cancers, and neuroblastomas [27–29]. In contrast, depending on the number and set of genes used for the determination of the CIMP status, the CIMP can be associated with either poor or good prognosis in GCs [30–33]. The CIMP in specific cancers is associated with genetic alterations, such as mutations of *BRAF*, *KRAS*, and *PIK3CA* in colorectal cancers [34–37], and amplification of *ERBB2* in breast cancers [38]. In contrast, little is known on a specific association between the CIMP and genetic alterations in GCs.

In this study, we aimed to establish integrated pictures of genetic and epigenetic alterations of GCs. To this end, we conducted comprehensive analysis of DNA methylation statuses using bead array technology, and extensive analysis of mutations of 55 known cancer-related genes using a next-generation personal sequencer.

2. Materials and methods

2.1. Samples

Thirty GC samples were obtained from patients who underwent gastrectomy with informed consents. Three normal gastric mucosae samples were obtained endoscopically from healthy volunteers without *H. pylori* infection with informed consents. The study was approved by the Institutional Review Boards. The samples were stored in RNAlater (Life Technologies, Carlsbad, CA) at −80 °C until the extraction of genomic DNA (GC samples and normal gastric mucosae samples) and RNA (normal gastric mucosae samples). Clinical information of the 30 GCs is shown in Supplementary Table 1. The status of Epstein–Barr (EB) virus infection was evaluated by PCR using primers specific to genomic DNA of EB virus (forward, CGGTATTATGTTTTTGGTATGTGTA; reverse, ATAACAACAACGTCATAAAAACCAC), and no infection was present in the 30 GCs.

Genomic DNA was extracted from GC and normal gastric mucosae samples by the phenol/chloroform method, and was quantified by using a Quant-iT PicoGreen dsDNA Assay Kit (Life Technologies). Total RNA was isolated using ISOGEN (Nippon Gene, Tokyo, Japan).

2.2. Analysis of DNA methylation

Analysis of DNA methylation was performed using an Infinium HumanMethylation450 BeadChip array, which covered 482,421 CpG sites (Illumina, San Diego, CA) as described previously [39]. CpG sites with low signals (signal <500, 0.19–2.19% of total CpG sites) were excluded from further analyses. The methylation level of each CpG site was represented by β values which ranged from 0 (unmethylated) to 1 (fully methylated).

A total of 193,531 genomic "segments" were defined by their location against a transcription start site (TSS) [TSS1500 (regions between 200 bp upstream and 1500 bp upstream from TSS), TSS200 (200 bp upstream region from TSS), 5′-UTR, 1st exon, gene body, 3′-UTR, and intergenic regions] and their relative location against a CGI (N Shelf, N Shore, CGI, S Shore, S Shelf, and non-CGI). A genomic segment >500 bp was further divided into genomic "blocks". A genomic block was defined as a 500-bp region from an initial CpG site (probe), and the next genomic block started from the next CpG site (Supplementary Fig. 1). A genomic segment ⩽500 bp was counted as one genomic block. A total of 282,805 genomic blocks were produced, and 276,456 genomic blocks on autosomes were analyzed to enable comparison between males and females. A DNA methylation level of a genomic block was evaluated using the average of β value of the CpG sites within the block. A genomic block was considered as methylated when its β value was 0.4 or more, and as unmethylated when its β value was 0.2 or less.

2.3. Analysis of sequence variations

A library DNA containing 226 amplicons of 55 cancer-related genes was prepared from a sample by multiplex PCR using 50 ng of genomic DNA and an Ion *AmpliSeq* Cancer Panel Kit (Life Technologies) with 36 customized primers (Supplementary Table 2). The 226 amplicons covered the vast majority of samples with mutations reported (91.9% or more) for 15 oncogenes and the *TP53* tumor-suppressor gene (83.1%), and variable fractions of samples with mutations reported (3.3–88.5%) for 39 genes (Supplementary Table 3). Then, the entire library DNA was uniquely barcoded by using an Ion Xpress Barcode Adaptors 1-16 Kit (Life Technologies). The barcoded libraries from five to six samples were pooled, and mixed with Ion Spheres for emulsion PCR using the Ion OneTouch System (Life Technologies) with an Ion OneTouch Template Kit (Life Technologies). From the product of emulsion PCR, the complexes of Ion Spheres with amplified DNA were enriched by using Ion OneTouch ES (Life Technologies) and were loaded onto an Ion 316 chip (Life Technologies). Sequencing was performed by using Ion PGM Sequencer (Life Technologies) with an Ion Sequencing Kit (Life Technologies). Obtained sequences were mapped onto the human reference genome hg19, and sequence variations with frequencies of 10% or more were identified by using CLC Genomics Workbench 5.1 (CLC bio, Aarhus, Denmark). Common SNPs were excluded from further analysis. Reading depths of individual regions analyzed are shown in Supplementary Table 4.

2.4. Dideoxy sequencing

A region containing a sequence variation identified was amplified using 20 ng of genomic DNA with primers listed in Supplementary Table 5. The PCR product was purified by a DNA Clean and Concentrator-5 Kit (Zymo Research, Irvine, CA), and directly cycle-sequenced by using a DYEnamic ET Terminator Cycle Sequencing kit (GE Healthcare, Buckinghamshire, UK) and an ABI PRISM 310 automated DNA sequencer (PE Biosystems).

2.5. Analysis of gene expression by GeneChip oligonucleotide microarray

Gene expression levels in normal gastric mucosae were analyzed by using the GeneChip Human Genome U133 Plus 2.0 microarray (Affymetrix, Santa Clara, CA) as described [40]. Genes with signal intensities of 250 or more were defined as expressed genes.

2.6. Cluster analysis

Unsupervised hierarchical clustering analysis was performed by using R 2.15 [R Core Team (2012) R: A language and environment for statistical computing. R Foundation for Statistical Computing, Vienna, Austria. ISBN 3-900051-07-0, URL http://www.R-project.org/] with the Heatplus package [Alexander Ploner (2011) Heatplus: Heatmaps with row and/or column covariates and colored clusters, R package version 2.2.0.] from Bioconductor [41]. The Euclidean distance was used as distance function both for samples and genes. Due to the limitation in the calculation algorithm for the hierarchical clustering, 25,000 elements or less were analyzed.

2.7. Survival curve

Survival curves were analyzed using the Kaplan-Meier method, and the Kaplan-Meier curve was drawn by using SPSS 13.0J (SPSS, Chicago, IL, USA).

2.8. Statistical analysis

The association between the CIMP and oncogene mutations, and that between genes aberrantly methylated in GCs and target genes of polycomb repressive complex (PRC) 2 in human embryonic stem (ES) cells were tested by the chi-square test. The differences in the survival rates among groups were evaluated using the Mantel-Cox test.

3. Results

3.1. Comprehensive analysis of DNA methylation profiles

DNA methylation levels were compared between GCs and normal gastric mucosae. First, using all the 276,456 genomic blocks, some GCs, such as S24TP, S33TP, and S37TP, had a larger fraction of aberrantly methylated blocks than other GCs, such as S2TP, S4TP, and S15TP (Fig. 1 and Supplementary Fig. 2). Second, the analysis was conducted using 6877 TSS200 CGIs unmethylated in normal gastric mucosae (genes unmethylated in normal gastric mucosae) because a TSS200 CGI is known to play a critical role in methylation-silencing [42]. The number of aberrantly methylated genes ranged from three to 1211. Third, we focused on TSS200 CGIs of genes with positive expression in normal cells but aberrantly methylated in cancer cells because this group of genes is known to frequently contain driver genes in carcinogenesis [43]. Using 263 TSS200 CGIs whose downstream genes were expressed in

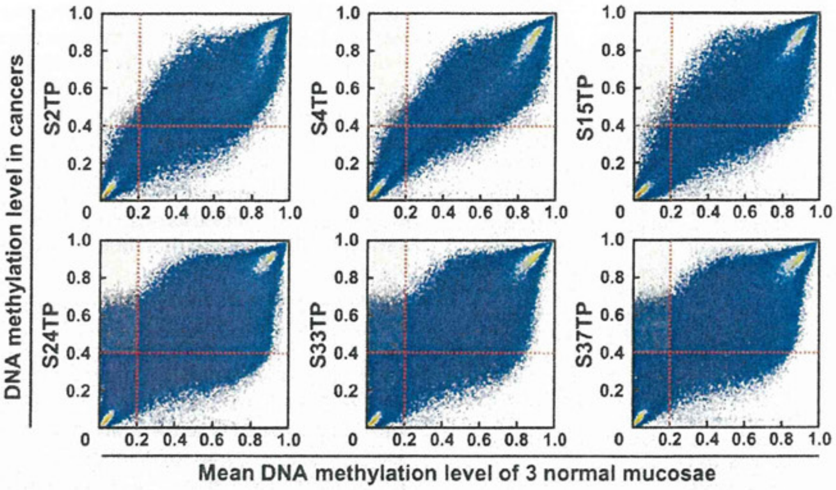

Fig. 1. Comprehensive analysis of DNA methylation profiles in GCs. DNA methylation levels were compared between GCs and normal gastric mucosae for the 276,456 genomic blocks. S24TP, S33TP, and S37TP (lower three panels) had a larger fraction of aberrantly methylated genes (yellow-colored areas) than S2TP, S4TP, and S15TP (upper three panels). The vertical and horizontal axes indicate the methylation levels in GCs and the mean methylation levels of three normal mucosae, respectively.

normal gastric mucosae and aberrantly methylated in one or more GCs (methylation-silenced genes), the number ranged from 0 to 166. These results showed that the number of aberrantly methylated genes was highly variable among individual GCs.

3.2. Extensive mutation analysis of the 55 cancer-related genes

Mutations were analyzed for the 55 cancer-related genes. Among the 30 GCs, 22 GCs had 30 sequence variations of at least one gene (Table 1 and Supplementary Table 6), and all the 30 sequence variations were confirmed by dideoxy sequencing (Supplementary Fig. 3). The confirmed sequence variations were analyzed whether or not they were somatic mutations using corresponding non-cancerous tissues. The 24 of the 30 sequence variations were shown to be somatic mutations (Fig. 2 and Table 1), and were present in 19 GCs. Among the 24 mutations, 22 were missense mutations, and two were nonsense mutations. Three GCs (S5TP, S13TP, and S33TP) had two or more mutations of different genes. Four oncogenes, *CTNNB1*, *ERBB2*, *KRAS*, and *PIK3CA*, and four tumor-suppressor genes, *CDH1*, *MLH1*, *SMARCB1*, and *TP53*, were mutated. *TP53* was most frequently mutated (43%, 13 of the 30 GCs), and *CTNNB1*, *ERBB2*, *KRAS*, and *PIK3CA* were mutated in two GCs. These results showed that 63% of GCs (19 out of the 30 GCs) had at least one somatic mutation of known cancer-related genes.

3.3. The association between the CIMP and mutations of oncogenes

Unsupervised hierarchical clustering analysis was conducted first using DNA methylation profiles of 25,000 genomic blocks randomly selected from all the 276,456 genomic blocks. However, the numbers of aberrantly methylated genes in GCs of different clusters did not appear to be different (Supplementary Fig. 4). Then, we again conducted unsupervised hierarchical clustering using DNA methylation profiles of CGIs, namely 25,000 genomic blocks randomly selected from 59,992 blocks with CGIs (Fig. 3A). This time, clusters I ($n = 3$) and IIb ($n = 13$) contained GCs with a larger number of aberrantly methylated genes than GCs in cluster IIa ($n = 14$). Among the 16 GCs in clusters I and IIb, seven GCs were shown to have mutations of oncogenes, *CTNNB1*, *ERBB2*, *KRAS*, and *PIK3CA*.

Thirdly, using DNA methylation profiles of 6877 genes unmethylated in normal gastric mucosae, two major clusters were observed (Fig. 3B). Cluster III ($n = 11$) contained GCs with a relatively large number of aberrantly methylated genes, and seven of the 11 GCs of this cluster were shown to have mutations of oncogenes, *CTNNB1*, *ERBB2*, *KRAS*, and *PIK3CA*. In contrast, cluster IV ($n = 19$) contained GCs with a relatively small number of aberrantly methylated genes, and none of the 19 GCs in this cluster had mutations of oncogenes. The difference was markedly statistically significant ($P = 7.15 \times 10^{-5}$), and GCs in cluster III and IV were considered to be the CIMP-positive [CIMP(+)] and the CIMP-negative [CIMP(−)], respectively.

Fourth, using DNA methylation profiles of the 263 methylation-silenced genes, three major clusters were produced (Fig. 3C). Cluster V ($n = 3$) contained GCs with the largest number of aberrantly methylated genes, and two of the three GCs were shown to have mutations of *PIK3CA*. Cluster VIa ($n = 8$) contained GCs with a relatively larger number of aberrantly methylated genes than GCs in cluster VIb ($n = 19$). Five of the eight GCs in this cluster were shown to have mutations of oncogenes, *CTNNB1*, *ERBB2*, *KRAS*. Clusters VIb contained the same sets of GCs as cluster IV, the previous clustering, except for one. These results showed that the CIMP(+) GCs were associated with mutations of oncogenes, such as *CTNNB1*, *ERBB2*, *KRAS* and *PIK3CA*, in GCs.

3.4. Possible association between the CIMP and good prognosis

To analyze an association between the CIMP status and prognosis of patients, Kaplan-Meier curves were drawn using overall survival (OS). Using the CIMP status based on the DNA methylation of the 6877 genes unmethylated in normal gastric mucosae, it was revealed that the prognosis of the CIMP(+) patients (Cluster III in Fig. 3B) tended to be better than that of the CIMP(−) patients (Cluster IV in Fig. 3B) ($P = 0.285$; Fig. 4). Also, using the CIMP status based on the methylation of the 263 methylation-silenced genes, the prognosis of the CIMP(+) patients (Cluster V and VIa in Fig. 3C) tended to be better than that of the CIMP(−) patients (Cluster VIb in Fig. 3C) ($P = 0.285$; Supplementary Fig. 5). These results suggested that the CIMP(+) status is possibly associated with good prognosis in GCs.

Table 1
List of somatic mutations identified in the 30 GCs.

Sample #	Sample name	Gene	Coverage	Variant frequencies	Nucleotide change	Amino acid change
1	S1TP	*CDH1*	339	10.3	c.1198G > A	p.Asp400Asn
2	S2TP	*TP53*	496	34.1	c.581T > G	p.Leu194Arg
3	S4TP	*TP53*	438	74.2	c.581T > G	p.Leu194Arg
4	S5TP	*KRAS*	1626	54.4	c.38G > A	p.Gly13Asp
		SMARCB1	50	56	c.1130G > A	p.Arg377His
5	S6TP	*TP53*	2077	24.7	c.820G > C	p.Val274Leu
6	S9TP			No mutation		
7	S11TP	*TP53*	10,211	53.4	c.844C > T	p.Arg282Trp
8	S12TP	*ERBB2*	24,516	63.8	c.2264T > C	p.Leu755Ser
9	S13TP	*TP53*	70	15.7	c.478A > G	p.Met160Val
		ERBB2	482	23.9	c.2264T > C	p.Leu755Ser
10	S14TP			No mutation		
11	S15TP	*TP53*	534	40.3	c.743G > A	p.Arg248Gln
12	S16TP	*TP53*	453	36.2	c.660T > G	p.Tyr220Ter
13	S17TP			No mutation		
14	S18TP	*TP53*	1946	26.5	c.844C > T	p.Arg282Trp
15	S19TP			No mutation		
16	S20TP			No mutation		
17	S22TP			No mutation		
18	S23TP	*TP53*	565	67.8	c.537T > A	p.His179Gln
19	S24TP			No mutation		
20	S32TP			No mutation		
21	S33TP	*MLH1*	4092	45.4	c.1744C > G	p.Leu582Val
		CTNNB1	11,994	20.5	c.101G > A	p.Gly34Glu
		PIK3CA	276	49.3	c.1633G > A	p.Glu545Lys
		TP53	1142	34.9	c.524G > A	p.Arg175His
22	S34TP	*TP53*	551	28.3	c.641A > G	p.His214Arg
23	S35TP	*KRAS*	770	41.3	c.35G > T	p.Gly12Val
24	S36TP	*TP53*	1142	34.9	c.524G > A	p.Arg175His
25	S37TP	*PIK3CA*	59	15.3	c.1624G > A	p.Glu542Lys
26	S40TP			No mutation		
27	S42TP			No mutation		
28	S43TP	*TP53*	239	74.9	c.1024C > T	p.Arg342Ter
29	S45TP			No mutation		
30	S47TP	*CTNNB1*	4591	33.7	c.121A > G	p.Thr41Ala

3.5. Association between the genes aberrantly methylated in GCs and genes targeted by PRC2 in ES cells

The fraction of genes targeted by PRC2 in ES cells was analyzed in the genes aberrantly methylated in GCs and those unmethylated in GCs because genes methylated in GCs were reported to be associated with PRC2 target genes [33]. Using the information on the PRC2 target genes in human ES cells [44,45], it was shown that the genes aberrantly methylated in GCs consisted of a larger fraction of PRC2 target genes than those unmethylated in GCs ($P = 6.64 \times 10^{-79}$) (Supplementary Fig. 6). These results confirmed that genes aberrantly methylated in GCs were associated with genes targeted by PRC2 in ES cells.

4. Discussion

In this study, we conducted comprehensive DNA methylation analysis and extensive mutation analysis of 30 GCs, and showed (1) that the number of aberrantly methylated genes was highly variable among the 30 GCs, (2) that 19 of the 30 GCs had 24 somatic mutations of 8 different genes (*CDH1*, *CTNNB1*, *ERBB2*, *KRAS*, *MLH1*, *PIK3CA*, *SMARCB1*, and *TP53*), and (3) that the CIMP was associated with mutations of oncogenes, including *ERBB2*, *CTNNB1*, *KRAS*, and *PIK3CA*, in GCs. This is one of the first studies in which both genetic and epigenetic alterations were extensively analyzed in the same set of samples, and the association between the CIMP and mutations of oncogenes in GCs was revealed here for the first time.

A similar association has been known also in colorectal cancers, but the mechanisms for this association are still unclear. As a possible mechanism, it has been proposed (1) that cancers with the CIMP can escape senescence caused by *BRAF* mutation owing to silencing of regulators of senescence by *BRAF* mutation, such as *IGFBP7* [46,47], and (2) that overexpression of the *BRAF* mutant can induce aberrant methylation at various genes, such as *MLH1* [48]. Similar possibilities can be hypothesized in GCs. As a mechanism for methylation induction by oncogenic mutation, if this applies to GCs, there is a possibility that oncogenic mutations displace factors involved in the susceptibility to methylation induction, such as RNA polymerase II [40,49–53].

Somatic mutations of four tumor-suppressor genes, *CDH1*, *MLH1*, *SMARCB1*, and *TP53*, and four oncogenes, *CTNNB1*, *ERBB2*, *KRAS*, and *PIK3CA*, were identified. Among these mutated genes, *TP53* (32%), *CDH1* (20%), *PIK3CA* (10%), *CTNNB1* (9%), *KRAS* (7%), and *ERBB2* (2%) are listed in the top 15 mutated genes in GCs in the Catalogue Of Somatic Mutations In Cancer (COSMIC) database. In contrast, mutations of *SMARCB1* have not been identified in GCs, even by whole exome sequencing [11,12], but were identified for the first time in this study, showing the usefulness of extensive mutation analysis of known cancer-related genes. *SMARCB1* encodes a component of chromatin remodeling complex, SWI/SNF, and is mutated in malignant rhabdoid tumors [54]. In GCs, the defects of components of SWI/SNF, such as mutation of *ARID1A* [11,12] and loss of BRM expression, are known [55]. Therefore, it is considered that the dysfunction of chromatin remodeling activity plays an important role in gastric carcinogenesis.

The selection of genomic blocks heavily influenced the results of unsupervised hierarchical clustering analysis. The association between the CIMP and mutations of oncogenes was clearly observed using DNA methylation profiles of the selected 6877 and 263 blocks, and some association was observed using the methylation profiles of the 25,000 blocks with CGIs. In contrast, no association was observed using the 25,000 blocks randomly selected from all the blocks. Therefore, it is considered that the selection of biologically important probes (or genes) is required to extract meaningful information from the huge amount of data obtained by comprehensive DNA methylation analysis.

We previously found that the CIMP statuses in GCs were not associated with DNA methylation statuses in background non-cancerous mucosae, contrary to expectations [30]. The presence of the CIMP(+) GCs suggested that CGIs methylated in GCs are composed of those methylated as a result of the CIMP and those methylated in background non-cancerous mucosae.

The genes aberrantly methylated in GCs here were associated with genes targeted by PRC2 in ES cells, confirming previous reports. It has been known that genes methylated in other types of cancers are associated with genes targeted by PRC2 in ES cells [49,50,53] or normal cells [40,50–52]. A recent comprehensive analysis in GCs also revealed that genes methylated in GCs were associated with genes targeted by PRC2 in ES cells [33]. EZH2, a component of PRC2, and CBX7, a component of PRC1, are known to interact with DNA methyltransferases [56,57], and these interactions seem to be a possible mechanism of the high frequency of DNA methylation of the genes targeted by PRC2.

The prognosis of the CIMP(+) patients tended to be better than that of the CIMP(−) patients. The association between the CIMP and prognosis is highly dependent upon cancer types. For example, the CIMP is associated with poor prognosis in colorectal cancers [28], lung cancers [29], and neuroblastoma [27]. In GCs, some studies showed association with good prognosis [30,31], and others showed that with poor prognosis [32,33]. The reason why the CIMP in GCs was associated with good prognosis in some studies is unknown, but it might be possible that genes involved

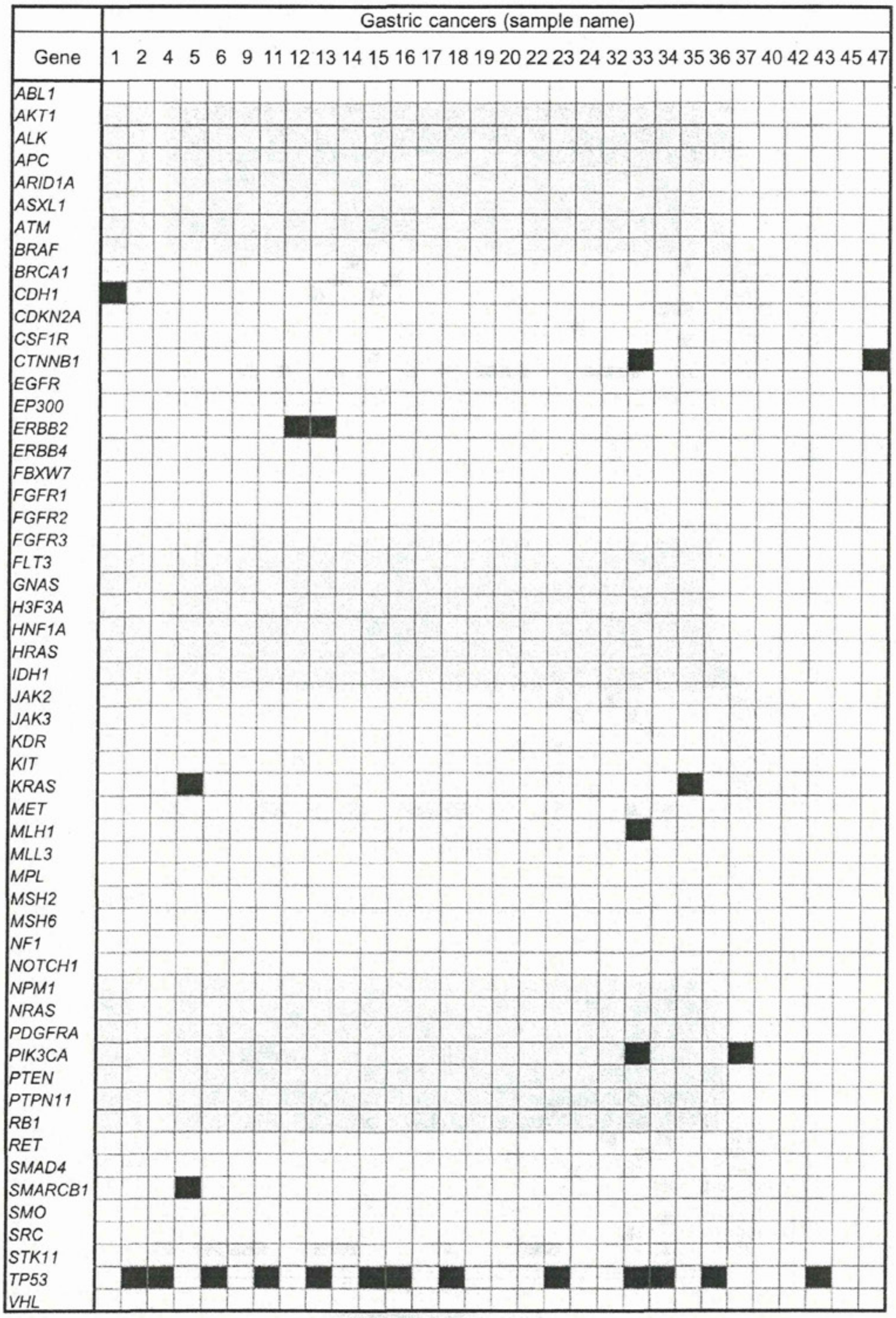

Fig. 2. Results of extensive mutation analysis of the 30 GCs. Mutations of the 55 known cancer-related genes were analyzed by Ion Torrent PGM sequencer. Among the 30 GCs, 19 had 24 somatic mutations of 8 different genes. *TP53* was mutated in 13 GCs (43%, 13 of the 30 GCs), and *CTNNB1*, *ERBB2*, *KRAS*, and *PIK3CA* were mutated in two GCs, respectively. The presence of a somatic mutation is shown by a filled square.

in tumor progression are silenced by aberrant DNA methylation in GCs with the CIMP.

In conclusion, integrated analysis of genetic and epigenetic alterations revealed that the CIMP was associated with mutations of oncogenes, including *ERBB2*, *CTNNB1*, *KRAS* and *PIK3CA*, in GCs.

Acknowledgements

This work was supported by Grants-in-Aid for the Third-Term Comprehensive Cancer Control Strategy from the Ministry of Health, Labour and Welfare, Japan, and by the A3 Foresight Program from the Japan Society for the Promotion of Science.

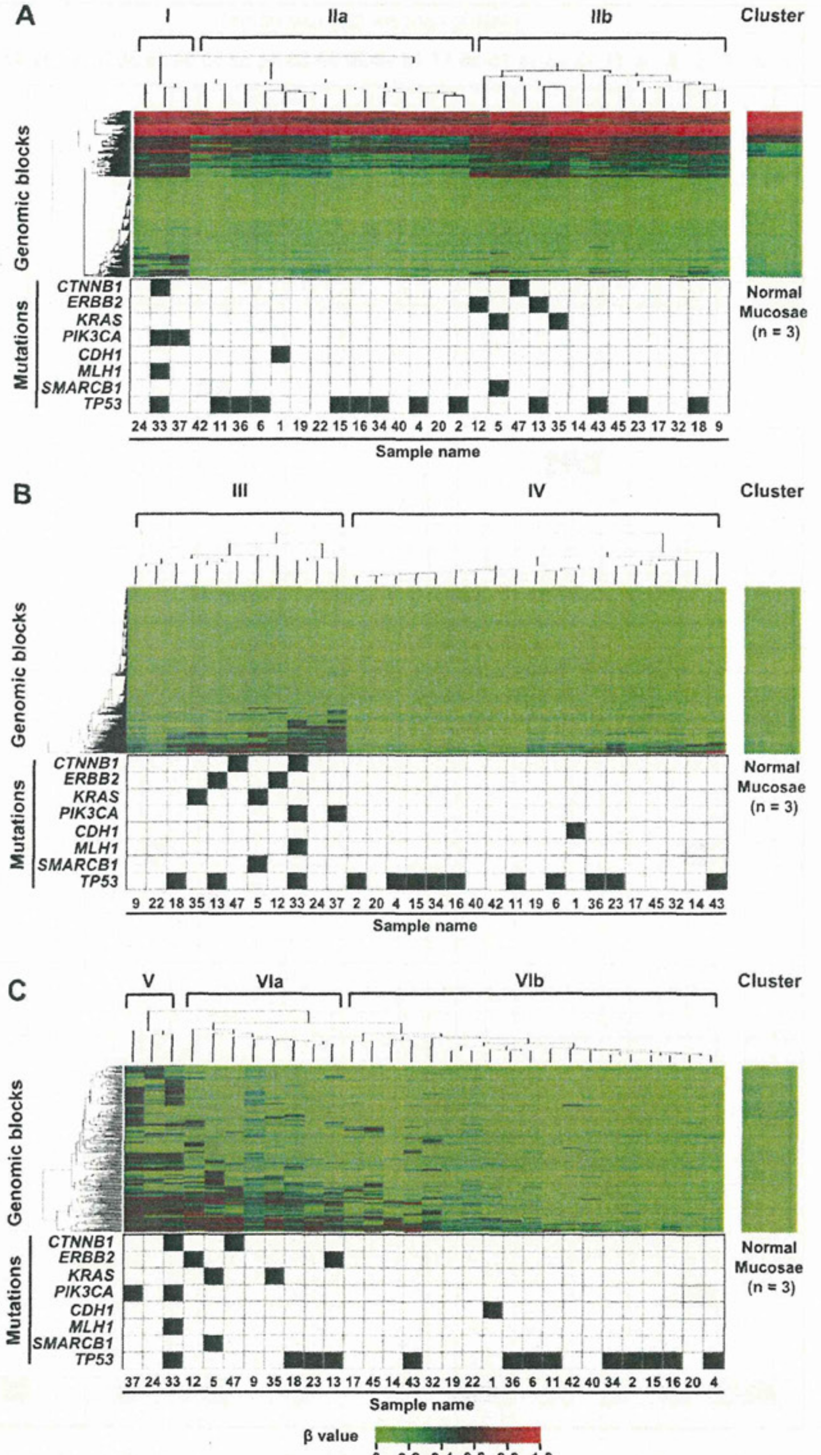

Fig. 3. The association between the DNA methylation profile and gene mutations. (A) Unsupervised hierarchical clustering analysis using DNA methylation profiles of 25,000 genomic blocks with CGIs. Clusters I ($n = 3$) and IIb ($n = 13$) contained GCs with a relatively large number of aberrantly methylated genes, and seven of the 16 GCs were shown to have mutations of oncogenes. (B) Unsupervised hierarchical clustering analysis using DNA methylation profiles of the 6877 blocks (genes) unmethylated in normal gastric mucosae. Cluster III ($n = 11$) contained GCs with a relatively large number of aberrantly methylated genes, and seven of the 11 GCs were shown to have mutations of oncogenes. (C) Unsupervised hierarchical clustering analysis using DNA methylation profiles of the 263 methylation-silenced genes. Cluster V ($n = 3$) contained GCs with the largest number of aberrantly methylated genes, and two of the three were shown to have *PIK3CA* mutations.

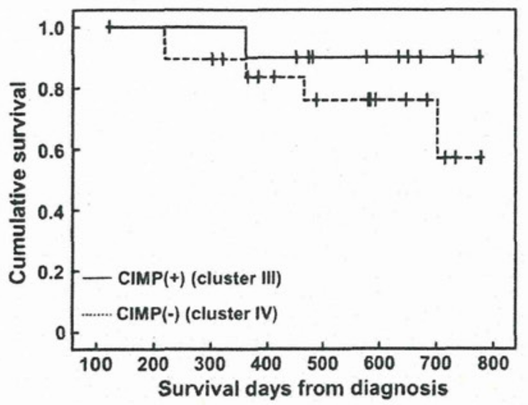

Fig. 4. The possible association between the CIMP and good prognosis. Kaplan-Meier curves were drawn using overall survival (OS). The CIMP status was determined based on the DNA methylation profile of the 6877 genes unmethylated in normal gastric mucosae. The prognosis of the CIMP(+) patients ($n = 11$) tended to be better than that of the CIMP(−) patients ($n = 19$) ($P = 0.285$).

Appendix A. Supplementary material

Supplementary data associated with this article can be found, in the online version, at http://dx.doi.org/10.1016/j.canlet.2012.11.022.

References

[1] M. Esteller, CpG island hypermethylation and tumor suppressor genes: a booming present, a brighter future, Oncogene 21 (2002) 5427–5440.
[2] I.A. Lea, M.A. Jackson, X. Li, S. Bailey, S.D. Peddada, J.K. Dunnick, Genetic pathways and mutation profiles of human cancers: site- and exposure-specific patterns, Carcinogenesis 28 (2007) 1851–1858.
[3] W.M. Clements, J. Wang, A. Sarnaik, O.J. Kim, J. MacDonald, C. Fenoglio-Preiser, J. Groden, A.M. Lowy, Beta-Catenin mutation is a frequent cause of Wnt pathway activation in gastric cancer, Cancer Res. 62 (2002) 3503–3506.
[4] M.A. Kim, E.J. Jung, H.S. Lee, H.E. Lee, Y.K. Jeon, H.K. Yang, W.H. Kim, Evaluation of *HER-2* gene status in gastric carcinoma using immunohistochemistry, fluorescence in situ hybridization, and real-time quantitative polymerase chain reaction, Hum. Pathol. 38 (2007) 1386–1393.
[5] V.S. Li, C.W. Wong, T.L. Chan, A.S. Chan, W. Zhao, K.M. Chu, S. So, X. Chen, S.T. Yuen, S.Y. Leung, Mutations of *PIK3CA* in gastric adenocarcinoma, BMC Cancer 5 (2005) 29.
[6] M. Nakajima, H. Sawada, Y. Yamada, A. Watanabe, M. Tatsumi, J. Yamashita, M. Matsuda, T. Sakaguchi, T. Hirao, H. Nakano, The prognostic significance of amplification and overexpression of c-met and c-erb B-2 in human gastric carcinomas, Cancer 85 (1999) 1894–1902.
[7] W.S. Park, R.R. Oh, J.Y. Park, S.H. Lee, M.S. Shin, Y.S. Kim, S.Y. Kim, H.K. Lee, P.J. Kim, S.T. Oh, N.J. Yoo, J.Y. Lee, Frequent somatic mutations of the beta-catenin gene in intestinal-type gastric cancer, Cancer Res. 59 (1999) 4257–4260.
[8] G. Suriano, N. Vrcelj, J. Senz, P. Ferreira, H. Masoudi, K. Cox, S. Nabais, C. Lopes, J.C. Machado, R. Seruca, F. Carneiro, D.G. Huntsman, Beta-catenin (CTNNB1) gene amplification: a new mechanism of protein overexpression in cancer, Genes Chromosom. Cancer 42 (2005) 238–246.
[9] S. Velho, C. Oliveira, A. Ferreira, A.C. Ferreira, G. Suriano, S. Schwartz Jr., A. Duval, F. Carneiro, J.C. Machado, R. Hamelin, R. Seruca, The prevalence of *PIK3CA* mutations in gastric and colon cancer, Eur. J. Cancer 41 (2005) 1649–1654.
[10] T. Yano, T. Doi, A. Ohtsu, N. Boku, K. Hashizume, M. Nakanishi, A. Ochiai, Comparison of *HER2* gene amplification assessed by fluorescence in situ hybridization and *HER2* protein expression assessed by immunohistochemistry in gastric cancer, Oncol. Rep. 15 (2006) 65–71.
[11] K. Wang, J. Kan, S.T. Yuen, S.T. Shi, K.M. Chu, S. Law, T.L. Chan, Z. Kan, A.S. Chan, W.Y. Tsui, S.P. Lee, S.L. Ho, A.K. Chan, G.H. Cheng, P.C. Roberts, P.A. Rejto, N.W. Gibson, D.J. Pocalyko, M. Mao, J. Xu, S.Y. Leung, Exome sequencing identifies frequent mutation of ARID1A in molecular subtypes of gastric cancer, Nat. Genet. 43 (2011) 1219–1223.
[12] Z.J. Zang, I. Cutcutache, S.L. Poon, S.L. Zhang, J.R. McPherson, J. Tao, V. Rajasegaran, H.L. Heng, N. Deng, A. Gan, K.H. Lim, C.K. Ong, D. Huang, S.Y. Chin, I.B. Tan, C.C. Ng, W. Yu, Y. Wu, M. Lee, J. Wu, D. Poh, W.K. Wan, S.Y. Rha, J. So, M. Salto-Tellez, K.G. Yeoh, W.K. Wong, Y.J. Zhu, P.A. Futreal, B. Pang, Y. Ruan, A.M. Hillmer, D. Bertrand, N. Nagarajan, S. Rozen, B.T. Teh, P. Tan, Exome sequencing of gastric adenocarcinoma identifies recurrent somatic mutations in cell adhesion and chromatin remodeling genes, Nat. Genet. 44 (2012) 570–574.
[13] M. Chan, S.M. Ji, Z.X. Yeo, L. Gan, E. Yap, Y.S. Yap, R. Ng, P.H. Tan, G.H. Ho, P. Ang, A.S. Lee, Development of a next-generation sequencing Method for BRCA mutation screening: a comparison between a high-throughput and a benchtop platform, J. Mol. Diagn. 14 (2012) 602–612.
[14] N.J. Loman, R.V. Misra, T.J. Dallman, C. Constantinidou, S.E. Gharbia, J. Wain, M.J. Pallen, Performance comparison of benchtop high-throughput sequencing platforms, Nat. Biotechnol. 30 (2012) 434–439.
[15] J. Sandoval, H. Heyn, S. Moran, J. Serra-Musach, M.A. Pujana, M. Bibikova, M. Esteller, Validation of a DNA methylation microarray for 450,000 CpG sites in the human genome, Epigenetics 6 (2011) 692–702.
[16] K. Asada, T. Ando, T. Niwa, S. Nanjo, N. Watanabe, E. Okochi-Takada, T. Yoshida, K. Miyamoto, S. Enomoto, M. Ichinose, T. Tsukamoto, S. Ito, M. Tatematsu, T. Sugiyama, T. Ushijima, FHL1 on chromosome X is a single-hit gastrointestinal tumor-suppressor gene and contributes to the formation of an epigenetic field defect, Oncogene (in press). http://dx.doi.org/10.1038/onc.2012.228.
[17] Y. Ding, X.P. Le, Q.X. Zhang, P. Du, Methylation and mutation analysis of p16 gene in gastric cancer, World J. Gastroenterol. 9 (2003) 423–426.
[18] D.C. Fang, R.Q. Wang, S.M. Yang, J.M. Yang, H.F. Liu, G.Y. Peng, T.L. Xiao, Y.H. Luo, Mutation and methylation of hMLH1 in gastric carcinomas with microsatellite instability, World J. Gastroenterol. 9 (2003) 655–659.
[19] A. Kaneda, K. Wakazono, T. Tsukamoto, N. Watanabe, Y. Yagi, M. Tatematsu, M. Kaminishi, T. Sugimura, T. Ushijima, Lysyl oxidase is a tumor suppressor gene inactivated by methylation and loss of heterozygosity in human gastric cancers, Cancer Res. 64 (2004) 6410–6415.
[20] J.C. Machado, C. Oliveira, R. Carvalho, P. Soares, G. Berx, C. Caldas, R. Seruca, F. Carneiro, M. Sobrinho-Simoes, E-cadherin gene (CDH1) promoter methylation as the second hit in sporadic diffuse gastric carcinoma, Oncogene 20 (2001) 1525–1528.
[21] M. Nojima, H. Suzuki, M. Toyota, Y. Watanabe, R. Maruyama, S. Sasaki, Y. Sasaki, H. Mita, N. Nishikawa, K. Yamaguchi, K. Hirata, F. Itoh, T. Tokino, M. Mori, K. Imai, Y. Shinomura, Frequent epigenetic inactivation of SFRP genes and constitutive activation of Wnt signaling in gastric cancer, Oncogene 26 (2007) 4699–4713.
[22] T. Ushijima, M. Sasako, Focus on gastric cancer, Cancer Cell 5 (2004) 121–125.
[23] T. Maekita, K. Nakazawa, M. Mihara, T. Nakajima, K. Yanaoka, M. Iguchi, K. Arii, A. Kaneda, T. Tsukamoto, M. Tatematsu, G. Tamura, D. Saito, T. Sugimura, M. Ichinose, T. Ushijima, High levels of aberrant DNA methylation in *Helicobacter pylori*-infected gastric mucosae and its possible association with gastric cancer risk, Clin. Cancer Res. 12 (2006) 989–995.
[24] T. Niwa, T. Tsukamoto, T. Toyoda, A. Mori, H. Tanaka, T. Maekita, M. Ichinose, M. Tatematsu, T. Ushijima, Inflammatory processes triggered by *Helicobacter pylori* infection cause aberrant DNA methylation in gastric epithelial cells, Cancer Res. 70 (2010) 1430–1440.
[25] N. Uemura, S. Okamoto, S. Yamamoto, N. Matsumura, S. Yamaguchi, M. Yamakido, K. Taniyama, N. Sasaki, R.J. Schlemper, *Helicobacter pylori* infection and the development of gastric cancer, N. Engl. J. Med. 345 (2001) 784–789.
[26] M. Toyota, N. Ahuja, M. Ohe-Toyota, J.G. Herman, S.B. Baylin, J.P. Issa, CpG island methylator phenotype in colorectal cancer, Proc. Natl. Acad. Sci. USA 96 (1999) 8681–8686.
[27] M. Abe, M. Ohira, A. Kaneda, Y. Yagi, S. Yamamoto, Y. Kitano, T. Takato, A. Nakagawara, T. Ushijima, CpG island methylator phenotype is a strong determinant of poor prognosis in neuroblastomas, Cancer Res. 65 (2005) 828–834.
[28] W.S. Samowitz, C. Sweeney, J. Herrick, H. Albertsen, T.R. Levin, M.A. Murtaugh, R.K. Wolff, M.L. Slattery, Poor survival associated with the BRAF V600E mutation in microsatellite-stable colon cancers, Cancer Res. 65 (2005) 6063–6069.
[29] K. Shinjo, Y. Okamoto, B. An, T. Yokoyama, I. Takeuchi, M. Fujii, H. Osada, N. Usami, Y. Hasegawa, H. Ito, T. Hida, N. Fujimoto, T. Kishimoto, Y. Sekido, Y. Kondo, Integrated analysis of genetic and epigenetic alterations reveals CpG island methylator phenotype associated with distinct clinical characters of lung adenocarcinoma, Carcinogenesis 33 (2012) 1277–1285.
[30] S. Enomoto, T. Maekita, T. Tsukamoto, T. Nakajima, K. Nakazawa, M. Tatematsu, M. Ichinose, T. Ushijima, Lack of association between CpG island methylator phenotype in human gastric cancers and methylation in their background non-cancerous gastric mucosae, Cancer Sci. 98 (2007) 1853–1861.
[31] M. Kusano, M. Toyota, H. Suzuki, K. Akino, F. Aoki, M. Fujita, M. Hosokawa, Y. Shinomura, K. Imai, T. Tokino, Genetic, epigenetic, and clinicopathologic features of gastric carcinomas with the CpG island methylator phenotype and an association with Epstein–Barr virus, Cancer 106 (2006) 1467–1479.
[32] S.Y. Park, M.C. Kook, Y.W. Kim, N.Y. Cho, N. Jung, H.J. Kwon, T.Y. Kim, G.H. Kang, CpG island hypermethylator phenotype in gastric carcinoma and its clinicopathological features, Virchows Arch. 457 (2010) 415–422.
[33] H. Zouridis, N. Deng, T. Ivanova, Y. Zhu, B. Wong, D. Huang, Y.H. Wu, Y. Wu, I.B. Tan, N. Liem, V. Gopalakrishnan, Q. Luo, J. Wu, M. Lee, W.P. Yong, L.K. Goh, B.T. Teh, S. Rozen, P. Tan, Methylation subtypes and large-scale epigenetic alterations in gastric cancer, Sci. Transl. Med. 4 (2012). 156ra140.
[34] K. Nosho, T. Kawasaki, M. Ohnishi, Y. Suemoto, G.J. Kirkner, D. Zepf, L. Yan, J.A. Longtine, C.S. Fuchs, S. Ogino, PIK3CA mutation in colorectal cancer: relationship with genetic and epigenetic alterations, Neoplasia 10 (2008) 534–541.
[35] M. Toyota, M. Ohe-Toyota, N. Ahuja, J.P. Issa, Distinct genetic profiles in colorectal tumors with or without the CpG island methylator phenotype, Proc. Natl. Acad. Sci. USA 97 (2000) 710–715.
[36] D.J. Weisenberger, K.D. Siegmund, M. Campan, J. Young, T.I. Long, M.A. Faasse, G.H. Kang, M. Widschwendter, D. Weener, D. Buchanan, H. Koh, L. Simms, M.

Barker, B. Leggett, J. Levine, M. Kim, A.J. French, S.N. Thibodeau, J. Jass, R. Haile, P.W. Laird, CpG island methylator phenotype underlies sporadic microsatellite instability and is tightly associated with BRAF mutation in colorectal cancer, Nat. Genet. 38 (2006) 787–793.

[37] V.L. Whitehall, C. Rickman, C.E. Bond, I. Ramsnes, S.A. Greco, A. Umapathy, D. McKeone, R.J. Faleiro, R.L. Buttenshaw, D.L. Worthley, S. Nayler, Z.Z. Zhao, G.W. Montgomery, K.A. Mallitt, J.R. Jass, N. Matsubara, K. Notohara, T. Ishii, B.A. Leggett, Oncogenic PIK3CA mutations in colorectal cancers and polyps, Int. J. Cancer 131 (2012) 813–820.

[38] K. Terada, E. Okochi-Takada, S. Akashi-Tanaka, K. Miyamoto, K. Taniyama, H. Tsuda, K. Asada, M. Kaminishi, T. Ushijima, Association between frequent CpG island methylation and HER2 amplification in human breast cancers, Carcinogenesis 30 (2009) 466–471.

[39] Y. Shigematsu, T. Niwa, S. Yamashita, H. Taniguchi, R. Kushima, H. Katai, S. Ito, T. Tsukamoto, M. Ichinose, T. Ushijima, Identification of a DNA methylation marker that detects the presence of lymph node metastases of gastric cancers, Oncol. Lett. 4 (2012) 268–274.

[40] H. Takeshima, S. Yamashita, T. Shimazu, T. Niwa, T. Ushijima, The presence of RNA polymerase II, active or stalled, predicts epigenetic fate of promoter CpG islands, Genome Res. 19 (2009) 1974–1982.

[41] R.C. Gentleman, V.J. Carey, D.M. Bates, B. Bolstad, M. Dettling, S. Dudoit, B. Ellis, L. Gautier, Y. Ge, J. Gentry, K. Hornik, T. Hothorn, W. Huber, S. Iacus, R. Irizarry, F. Leisch, C. Li, M. Maechler, A.J. Rossini, G. Sawitzki, C. Smith, G. Smyth, L. Tierney, J.Y. Yang, J. Zhang, Bioconductor: open software development for computational biology and bioinformatics, Genome Biol. 5 (2004) R80.

[42] J.C. Lin, S. Jeong, G. Liang, D. Takai, M. Fatemi, Y.C. Tsai, G. Egger, E.N. Gal-Yam, P.A. Jones, Role of nucleosomal occupancy in the epigenetic silencing of the MLH1 CpG island, Cancer Cell 12 (2007) 432–444.

[43] M. Kikuyama, H. Takeshima, T. Kinoshita, E. Okochi-Takada, M. Wakabayashi, S. Akashi-Tanaka, T. Ogawa, Y. Seto, T. Ushijima, Development of a novel approach, the epigenome-based outlier approach, to identify tumor-suppressor genes silenced by aberrant DNA methylation, Cancer Lett. 322 (2012) 204–212.

[44] I. Ben-Porath, M.W. Thomson, V.J. Carey, R. Ge, G.W. Bell, A. Regev, R.A. Weinberg, An embryonic stem cell-like gene expression signature in poorly differentiated aggressive human tumors, Nat. Genet. 40 (2008) 499–507.

[45] T.I. Lee, R.G. Jenner, L.A. Boyer, M.G. Guenther, S.S. Levine, R.M. Kumar, B. Chevalier, S.E. Johnstone, M.F. Cole, K. Isono, H. Koseki, T. Fuchikami, K. Abe, H.L. Murray, J.P. Zucker, B. Yuan, G.W. Bell, E. Herbolsheimer, N.M. Hannett, K. Sun, D.T. Odom, A.P. Otte, T.L. Volkert, D.P. Bartel, D.A. Melton, D.K. Gifford, R. Jaenisch, R.A. Young, Control of developmental regulators by Polycomb in human embryonic stem cells, Cell 125 (2006) 301–313.

[46] T. Hinoue, D.J. Weisenberger, F. Pan, M. Campan, M. Kim, J. Young, V.L. Whitehall, B.A. Leggett, P.W. Laird, Analysis of the association between CIMP and BRAF in colorectal cancer by DNA methylation profiling, PLoS ONE 4 (2009) e8357.

[47] H. Suzuki, S. Igarashi, M. Nojima, R. Maruyama, E. Yamamoto, M. Kai, H. Akashi, Y. Watanabe, H. Yamamoto, Y. Sasaki, F. Itoh, K. Imai, T. Sugai, L. Shen, J.P. Issa, Y. Shinomura, T. Tokino, M. Toyota, IGFBP7 is a p53-responsive gene specifically silenced in colorectal cancer with CpG island methylator phenotype, Carcinogenesis 31 (2010) 342–349.

[48] P. Minoo, M.P. Moyer, J.R. Jass, Role of BRAF-V600E in the serrated pathway of colorectal tumourigenesis, J. Pathol. 212 (2007) 124–133.

[49] J.E. Ohm, K.M. McGarvey, X. Yu, L. Cheng, K.E. Schuebel, L. Cope, H.P. Mohammad, W. Chen, V.C. Daniel, W. Yu, D.M. Berman, T. Jenuwein, K. Pruitt, S.J. Sharkis, D.N. Watkins, J.G. Herman, S.B. Baylin, A stem cell-like chromatin pattern may predispose tumor suppressor genes to DNA hypermethylation and heritable silencing, Nat. Genet. 39 (2007) 237–242.

[50] Y. Schlesinger, R. Straussman, I. Keshet, S. Farkash, M. Hecht, J. Zimmerman, E. Eden, Z. Yakhini, E. Ben-Shushan, B.E. Reubinoff, Y. Bergman, I. Simon, H. Cedar, Polycomb-mediated methylation on Lys27 of histone H3 pre-marks genes for de novo methylation in cancer, Nat. Genet. 39 (2007) 232–236.

[51] H. Takeshima, T. Ushijima, Methylation destiny: Moira takes account of histones and RNA polymerase II, Epigenetics 5 (2010) 89–95.

[52] H. Takeshima, S. Yamashita, T. Shimazu, T. Ushijima, Effects of genome architecture and epigenetic factors on susceptibility of promoter CpG islands to aberrant DNA methylation induction, Genomics 98 (2011) 182–188.

[53] M. Widschwendter, H. Fiegl, D. Egle, E. Mueller-Holzner, G. Spizzo, C. Marth, D.J. Weisenberger, M. Campan, J. Young, I. Jacobs, P.W. Laird, Epigenetic stem cell signature in cancer, Nat. Genet. 39 (2007) 157–158.

[54] B.G. Wilson, C.W. Roberts, SWI/SNF nucleosome remodellers and cancer, Nat. Rev. Cancer 11 (2011) 481–492.

[55] N. Yamamichi, K. Inada, M. Ichinose, M. Yamamichi-Nishina, T. Mizutani, H. Watanabe, K. Shiogama, M. Fujishiro, T. Okazaki, N. Yahagi, T. Haraguchi, S. Fujita, Y. Tsutsumi, M. Omata, H. Iba, Frequent loss of Brm expression in gastric cancer correlates with histologic features and differentiation state, Cancer Res. 67 (2007) 10727–10735.

[56] H.P. Mohammad, Y. Cai, K.M. McGarvey, H. Easwaran, L. Van Neste, J.E. Ohm, H.M. O'Hagan, S.B. Baylin, Polycomb CBX7 promotes initiation of heritable repression of genes frequently silenced with cancer-specific DNA hypermethylation, Cancer Res. 69 (2009) 6322–6330.

[57] E. Vire, C. Brenner, R. Deplus, L. Blanchon, M. Fraga, C. Didelot, L. Morey, A. Van Eynde, D. Bernard, J.M. Vanderwinden, M. Bollen, M. Esteller, L. Di Croce, Y. de Launoit, F. Fuks, The Polycomb group protein EZH2 directly controls DNA methylation, Nature 439 (2006) 871–874.

Carcinogenesis vol.33 no.12 pp.2384–2390, 2012
doi:10.1093/carcin/bgs294
Advance Access publication September 13, 2012

Induction of aberrant trimethylation of histone H3 lysine 27 by inflammation in mouse colonic epithelial cells

Hideyuki Takeshima, Daigo Ikegami, Mika Wakabayashi, Tohru Niwa, Young-Joon Kim[1] and Toshikazu Ushijima*

Division of Epigenomics, National Cancer Center Research Institute, 5-1-1 Tsukiji, Chuo-ku, 104-0045, Tokyo, Japan and [1]Department of Biochemistry, Genome Regulation Center, Yonsei University, Seoul, Korea

*To whom correspondence should be addressed. Fax: +81 3 5565 1753; Email: tushijim@ncc.go.jp

A field for cancerization (field defect), where genetic and epigenetic alterations are accumulated in normal-appearing tissues, is involved in human carcinogenesis, especially cancers associated with chronic inflammation. Although aberrant DNA methylation is involved in the field defect and induced by chronic inflammation, it is still unclear for trimethylation of histone H3 lysine 27 (H3K27me3), which is involved in gene repression independent of DNA methylation and functions as a pre-mark for aberrant DNA methylation. In this study, using a mouse colitis model induced by dextran sulfate sodium (DSS), we aimed to clarify whether aberrant H3K27me3 is induced by inflammation and involved in a field defect. ChIP-on-chip analysis of colonic epithelial cells revealed that H3K27me3 levels were increased or decreased for 266 genomic regions by aging, and more extensively (23 increased and 3574 decreased regions) by colitis. Such increase or decrease of H3K27me3 was induced as early as 2 weeks after the initiation of DSS treatment, and persisted at least for 16 weeks even after the inflammation disappeared. Some of the aberrant H3K27me3 in colonic epithelial cells was carried over into colon tumors. Furthermore, H3K27me3 acquired at *Dapk1* by colitis was followed by increased DNA methylation, supporting its function as a pre-mark for aberrant DNA methylation. These results demonstrated that aberrant H3K27me3 can be induced by exposure to a specific environment, such as colitis, and suggested that aberrant histone modification, in addition to aberrant DNA methylation, is involved in the formation of a field defect.

Introduction

A field for cancerization (field defect) is known as normal-appearing tissues predisposed to carcinogenesis, and is deeply involved in development of human cancers, especially those associated with chronic inflammation, such as gastric cancers (1). The predisposition is considered to be due to accumulation of genetic and epigenetic alterations (2,3). Although the frequencies of genetic alterations in normal-appearing tissues are too low to be accurately measured (4), high levels of aberrant DNA methylation can be present in normal-appearing tissues and the levels can be correlated with risk of cancer development (epigenetic field defect) (3). DNA methylation in normal-appearing tissues is now known to be induced by aging (5–7) and exposure to specific carcinogenic factors, represented by chronic inflammation (8–10).

Epigenetic modifications consist of not only DNA methylation but also histone modifications (11), which are involved in both gene repression and activation and have various biological functions (12,13). Among histone modifications, trimethylation of histone H3 lysine 27 (H3K27me3) is involved in gene repression, independently of DNA methylation (14). Aberrant H3K27me3 is frequently observed in various cancers (14–16), and is involved in repression of tumor-suppressor genes such as *CDH1* (E-cadherin) and *RUNX3* (17,18). H3K27me3 is also important as a pre-mark in normal cells of genes in which aberrant DNA methylation is induced during carcinogenesis (19–24). Nevertheless, in contrast with the clear involvement of aberrant DNA methylation in the formation of an epigenetic field defect, the involvement of aberrant histone modifications is currently unknown. In addition, although induction of aberrant H3K27me3 by cobalt compounds and cigarette smoke condensate has been reported in cultured cells (25,26), its inducers *in vivo* are unknown.

In this study, we aimed to clarify whether aberrant H3K27me3 is induced in normal-appearing tissues by exposure to a specific environment and can be involved in an epigenetic field defect. To this end, we used a mouse colitis model induced by dextran sulfate sodium (DSS) because we previously demonstrated that aberrant DNA methylation can be induced at an early stage in this model (27).

Materials and methods

Animals and induction of inflammation and colon tumors

Male BALB/c mice were purchased from Charles River Laboratories (Yokohama, Japan). To induce colitis, 7-week-old mice were given DSS (molecular weight = 36 000–50 000; MP Biochemicals, Solon, OH) in drinking water at a concentration of 2.0% (wt/vol) for 1 week. To induce colon tumors, BALB/c mice were intraperitoneally injected with 10 mg/kg body weight of azoxymethane (NARD Institute, Amagasaki, Japan) and given DSS in drinking water (27), and tumors were obtained at 15 weeks after the initiation of DSS treatment. Colonic epithelial cells were isolated from distal large bowels by the crypt isolation technique (27). For the analysis of expression of inflammation-related genes, the entire colon, including both colonic mucosae and muscle layer, was used. All the animal experiments were approved by the Committee for Ethics in Animal Experimentation at the National Cancer Center.

Chromatin immunoprecipitation

As described previously (23), 10 μg of chromatin extracted from cross-linked colonic epithelial cells or colon tumor cells was immunoprecipitated by using 2 μg of specific antibodies [H3K27me3 (07-449, Millipore, Billerica, MA), H3K9me2 (308-32361, Wako, Osaka, Japan) and H3K9me3 (301-34833, Wako)] and Dynabeads Protein A (Invitrogen Dynal AS, Oslo, Norway). After reversal of cross-link, DNA was recovered with RNaseA and proteinase K treatment, followed by phenol/chloroform extraction and isopropanol precipitation. Recovered DNA was dissolved in 33 μl of 1 × TE (10 mM Tris-HCl and 1 mM ethylenediaminetetraacetic acid).

One microliter of immunoprecipitated and input DNA was used for real-time chromatin immunoprecipitation (ChIP)–quantitative PCR (ChIP-qPCR). ChIP-qPCR was performed as described (23) with primers listed in Supplementary Table 1, available at *Carcinogenesis* Online. The numbers of DNA molecules in input and immunoprecipitated samples were obtained by comparing its amplification curve with those of standard samples with known numbers of DNA molecules. The specificity of the ChIP assay was confirmed by using primers for control regions (Supplementary Figure 1, available at *Carcinogenesis* Online).

Microarray analysis

Five hundred nanograms of immunoprecipitated and input DNA were labeled with Cy5 and Cy3, respectively, and hybridized with a mouse CpG island (CGI) oligonucleotide microarray (Agilent Technologies, Santa Clara, CA). Microarray scanning and data processing were performed as described (23,28), and the obtained signal ratio [Cy5 signal (bound)/Cy3 signal (input)] was normalized by the median of signal ratios of all probes. The H3K27me3 level of a region was evaluated using the average of signal ratios of the probes within the region. Genomic regions were defined as an assembly of probes with intervals <500 bp, and a region spanning both a promoter and gene body was split into two regions. Regions with only one or two probes were excluded from the analysis, and 16 126 regions were analyzed. When H3K27me3 levels in two samples were compared, we selected regions that showed a decrease or increase of 1.5-fold or more and had H3K27me3 levels higher than 1.5 in at least one sample.

Abbreviations: CGI, CpG island; ChIP, chromatin immunoprecipitation; DSS, dextran sulfate sodium; FACS, fluorescence-activated cell sorting; H3K27me3, trimethylation of histone H3 lysine 27; qRT-PCR, quantitative reverse transcription-PCR.

Fluorescence-activated cell sorting

Colonic epithelial cells obtained from three mice were incubated in Hanks' balanced salt solution containing 10 mM *N*-2-hydroxyethylpiperazine-*N'*-2-ethanesulfonic acid (pH 7.3), 1 mg/ml collagenase D (Roche Diagnostics, Penzberg, Germany) and 5 μg/ml DNase I (Sigma–Aldrich, St Louis, MO) at 37°C for 20 min with gentle agitation. Dispersed epithelial cells were treated with 1% formaldehyde at 30°C for 10 min and filtered with a cell strainer (BD, Franklin Lakes, NJ). The cross-linked cells were incubated with a phycoerythrin-labeled anti-mouse Epcam antibody (eBioscience, San Diego, CA) and a fluorescein isothiocyanate-labeled anti-Cd45 antibody (Miltenyi Biotech, Auburn, CA), and sorted using FACSAria II cell sorter (BD).

Quantitative reverse transcription-PCR

Total RNA was isolated using ISOGEN (Nippon Gene, Tokyo, Japan). cDNA was synthesized from 1 μg of total RNA using SuperScript III reverse transcriptase and an oligo $(dT)_{12-18}$ primer (Invitrogen, Carlsbad, CA). Quantitative reverse transcription-PCR (qRT-PCR) was performed as described (10) using primers listed in Supplementary Table 2, available at *Carcinogenesis* Online. The number of target cDNA molecules was normalized to that of *Gapdh* cDNA molecules.

Quantitative methylation-specific PCR

One microgram of *Bam*HI-digested genomic DNA was treated with sodium bisulfite as described (29). Bisulfite-treated DNA was re-suspended in 40 μl of 1 × TE, and 1 μl was used for quantitative methylation-specific PCR using primers specific to methylated target loci and to B2 SINE repeat (Supplementary Table 3, available at *Carcinogenesis* Online). DNA methylation levels were expressed as the percentage of methylation reference (27,30). Percentage of methylation reference was calculated as [(number of molecules methylated at a target region in a sample)/(number of B2 SINE repeat in the sample)]/[(number of molecules methylated at the target region in fully methylated DNA)/(number of B2 SINE repeat in the fully methylated DNA)] × 100. Genomic DNA treated with *SssI* methylase (New England Biolabs, Beverly, MA) was used as fully methylated DNA.

Results

Alterations of H3K27me3 levels were induced by aging, and more extensively by colitis

First, age-associated alterations of H3K27me3 levels were searched for by ChIP-CGI microarray (ChIP-on-chip) analysis of colonic epithelial cells obtained from 7-week-old mice and those from 23-week-old mice (Figure 1A and 1B). Among the 16 126 regions analyzed, H3K27me3 levels of 243 and 23 regions were increased and decreased, respectively. Then, colitis-associated alterations of H3K27me3 levels were searched for by comparing H3K27me3 levels between colonic epithelial cells of 23-week-old mice exposed to DSS-induced colitis and those of age-matched mock-treated mice (Figure 1A and 1C). H3K27me3 levels of 27 and 3782 regions were increased and decreased, respectively, by colitis. Among the 3809 regions with alterations, 212 regions overlapped with those whose alterations were induced by aging (Figure 1D). For the remaining 3597 regions, H3K27me3 levels of 23 (including 7 promoters and 15 gene bodies) and 3574 (including 866 promoters and 1934 gene bodies) regions were increased and decreased, respectively (Figure 1E).

The data obtained by ChIP-on-chip analysis were confirmed by ChIP-qPCR using 21 regions with H3K27me3-level alterations of 1.5-fold or more and four regions with alterations of 1.5-fold or less (Supplementary Table 4, available at *Carcinogenesis* Online). Alterations of the H3K27me3 levels obtained by both methods were well correlated ($r = 0.71$, Supplementary Figure 2, available at *Carcinogenesis* Online). These results showed that most alterations in H3K27me3 levels detected by ChIP-on-chip could be confirmed by ChIP-qPCR, and such alterations could be induced by exposure to colitis.

Since H3K27me3 alterations were extensive, we analyzed alterations of other well-known repressive histone modifications, H3K9me2 and H3K9me3 (12). As with the case of H3K27me3, large numbers of regions showed alterations of these two modifications (Supplementary Figure 3A–D, available at *Carcinogenesis* Online). Notably, regions with H3K27me3-level alterations hardly overlapped with regions with either H3K9me2- or H3K9me3-level alterations (Supplementary Figure 3E and F, available at *Carcinogenesis* Online).

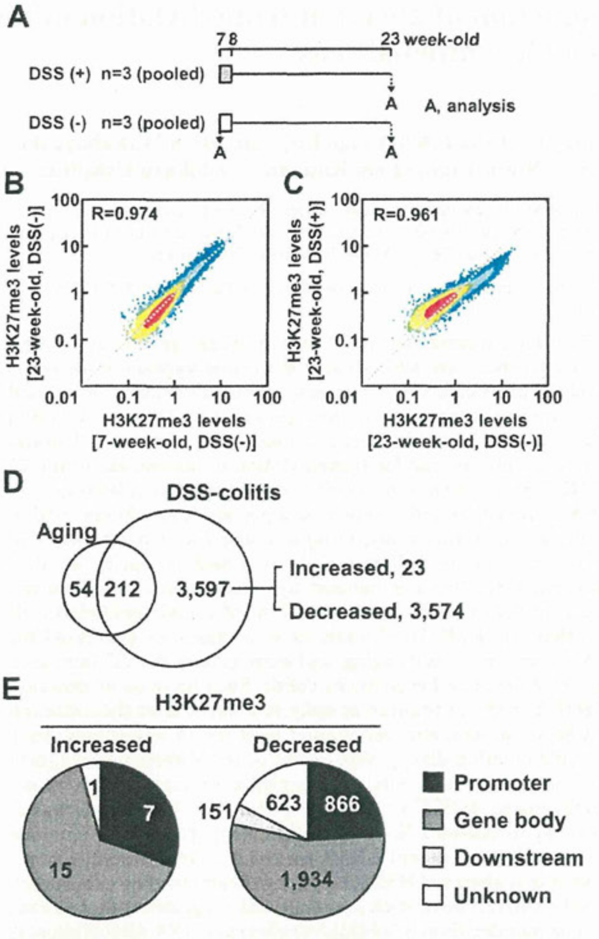

Fig. 1. Identification of genomic regions whose H3K27me3 levels were altered by aging and exposure to DSS-induced colitis. (**A**) Experimental protocol of sample preparation for ChIP-on-chip. (**B**) Alterations of the H3K27me3 levels in colonic epithelial cells by aging. Among the 16 126 regions analyzed, H3K27me3 levels of 243 and 23 regions were increased and decreased, respectively, at 1.5-fold or more by aging. (**C**) Alterations of the H3K27me3 levels by colitis. H3K27me3 levels of 27 and 3782 regions were increased and decreased, respectively, at 1.5-fold or more. (**D**) The overlap of regions whose H3K27me3 levels were altered by aging and those by colitis. Among the 3597 regions specifically altered by colitis, 23 and 3574 regions showed increased and decreased, respectively, H3K27me3 levels. (**E**) Classification of regions with H3K27me3-level alterations. Regions were classified into promoter (within 10 kb upstream of the transcription start site), gene body and downstream (within 10 kb downstream from genes) regions. Twenty-three regions with increased H3K27me3 levels contained 7 promoters and 15 gene bodies, respectively, and 3574 regions with decreased H3K27me3 levels contained 866 promoters and 1934 gene bodies, respectively. Regions that could not be classified by these criteria are indicated as unknown.

Aberrant H3K27me3 was induced at early stage, and remained for a long term even after its inducer disappeared

The temporal profiles of H3K27me3 levels in the course of DSS treatment were analyzed using 10 regions that showed alterations of 2-fold or more by ChIP-qPCR (Figure 2A). Among the six regions whose H3K27me3 levels were increased at 16 weeks (23-week-old mice) from the initiation of DSS treatment, three regions (*Abca1*, *Dapk1* and *Gramd1b*) showed significant increase of H3K27me3 levels at 2 weeks (Figure 2B). Similarly, among the four regions whose H3K27me3 levels were decreased at 16 weeks, two regions [*B4galnt1* (CGI2300) and *Plcd3*] showed significant decrease of H3K27me3 levels at 2

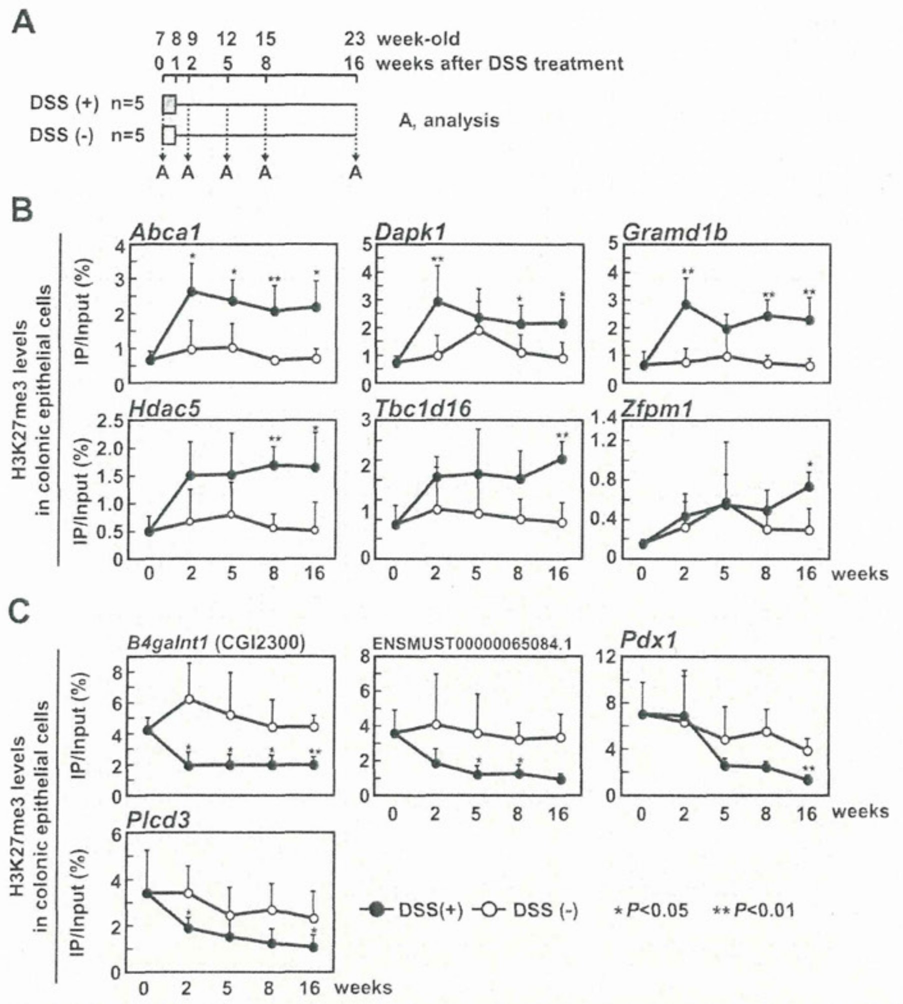

Fig. 2. Temporal profiles of H3K27me3 levels in the course of DSS-induced colitis. (**A**) Experimental protocol of preparation of colonic epithelial cells for ChIP-qPCR. (**B**) Analysis of genomic regions with increased H3K27me3. H3K27me3 levels of *Abca1*, *Dapk1* and *Gramd1b* were significantly increased at 2 weeks, and alterations persisted for at least 16 weeks, whereas those of *Hdac5*, *Tbc1d16* and *Zfpm1* were significantly increased only at late phases of colitis. Black and white circles show DSS-treated ($n = 5$) and mock-treated ($n = 5$) groups, respectively. The significance of difference was evaluated by the Mann–Whitney *U*-test ($*P < 0.05$, $**P<0.01$). (**C**) Analysis of genomic regions with decreased H3K27me3. H3K27me3 levels of *B4galnt1* (CGI2300) and *Plcd3* were significantly decreased at 2 weeks, and alterations persisted at least for 16 weeks. Those of ENSMUST00000065084.1 and *Pdx1* were significantly decreased only at late phase of colitis.

weeks (Figure 2C). Alterations in the H3K27me3 levels in these regions persisted at least until 16 weeks. Similar alterations in the H3K27me3 levels were confirmed in fluorescence-activated cell sorting (FACS)-purified colonic epithelial cells (Supplementary Figure 4, available at *Carcinogenesis* Online).

Temporal profiles of inflammation were then analyzed by examining expression of inflammation-related genes, *Il1b*, *Nos2* and *Tnf*, which are known to be upregulated in DSS-induced mouse colitis (27). Although the three genes were significantly upregulated at 2 and 5 weeks, their upregulation disappeared at 8 and 16 weeks (Figure 3A). Temporal profiles of expression of genes involved in the regulation of H3K27me3 were then analyzed. Expression levels of components of PRC2 (*Ezh2*, *Eed* and *Suz12*), PRC1 (*Bmi1*, *Ring1* and *Rnf2*) and H3K27 demethylases (*Kdm6a* and *Kdm6b*) were not altered by exposure to DSS-induced colitis (Figure 3B). These results indicated that aberrant H3K27me3 was induced at an early stage of colitis, and remained for the long term even after its inducer, inflammation, disappeared.

Altered H3K27me3 levels were associated with altered gene expression

The association between the altered H3K27me3 levels and altered gene expression was examined by temporal analysis of gene expression in colonic epithelial cells. Genes with increased H3K27me3 levels, *Dapk1* (gene body), *Gramd1b* (gene body), *Hdac5* (gene body), *Tbc1d16* (gene body) and *Zfpm1* (promoter), had decreased gene expression (Figure 4A). Among these genes, *Dapk1*, *Gramd1b* and *Tbc1d16* expression decreased at 5 weeks, but *Hdac5* and *Zfpm1* expression decreased at late phases of colitis. In contrast, genes with decreased H3K27me3 levels, *B4galnt1* (gene body), *Pdx1* (gene body) and *Plcd3* (gene body), had increased gene expression at 2 weeks (Figure 4B). These results indicated that altered H3K27me3 levels were associated with altered gene expression.

Some of the aberrant H3K27me3 were present in DSS-induced tumors

Alterations functionally involved in carcinogenesis are probably present also in tumor tissues. Therefore, we examined alterations of the H3K27me3 levels in colon tumors induced by azoxymethane and

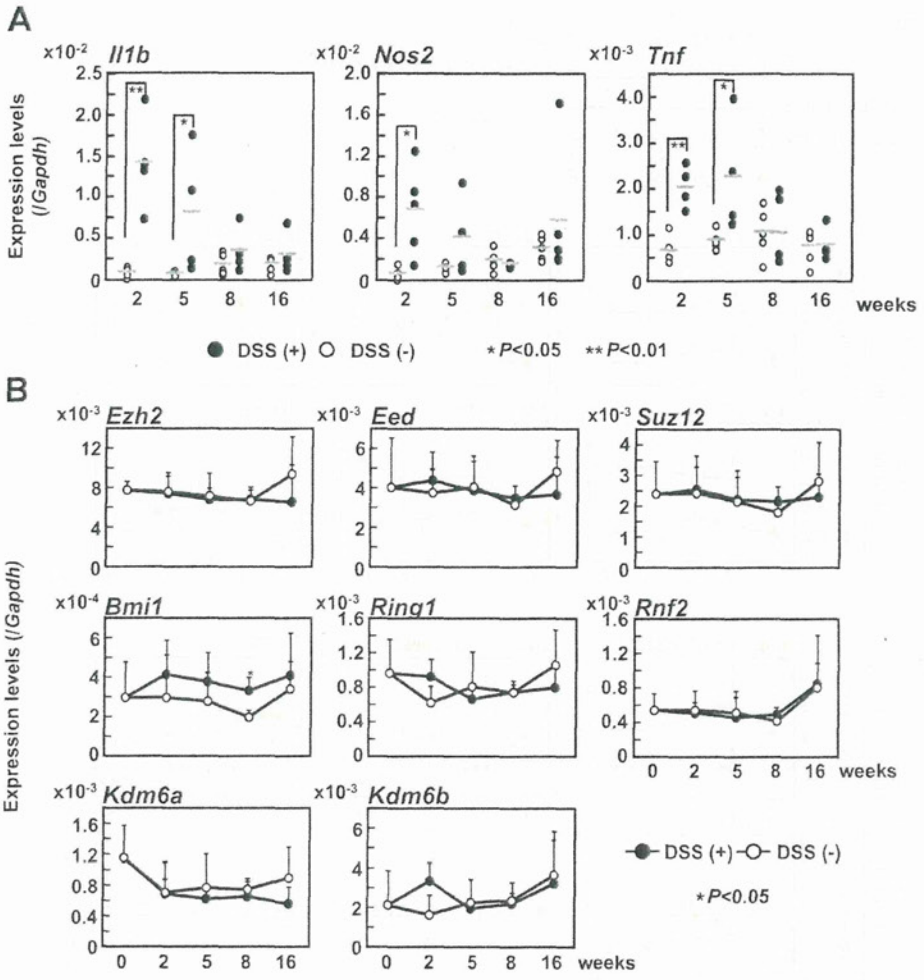

Fig. 3. Temporal profiles of expression of inflammation-related genes and polycomb-related genes in the course of DSS-induced colitis. (**A**) Temporal profiles of expression of inflammation-related genes. Gene expression was analyzed in samples of the entire colon by qRT-PCR. *Il1b*, *Nos2* and *Tnf* were upregulated at 2 and 5 weeks, but the upregulation disappeared at 8 and 16 weeks. Black and white circles show DSS-treated ($n = 5$) and mock-treated ($n = 5$) groups, respectively. The significance of difference was evaluated by the Mann–Whitney *U*-test ($*P < 0.05$, $**P<0.01$). (**B**) Temporal profiles of expression of polycomb-related genes. Gene expression was analyzed in colonic epithelial cells by qRT-PCR. Expression levels of these genes were not altered by exposure to DSS-induced colitis.

DSS. *Dapk1* and *Gramd1b* showed higher levels in colon tumors than those in mock-treated normal colonic epithelial cells whereas *Abca1*, *Hdac5*, *Tbc1d16* and *Zfpm1* did not. On the other hand, *B4galnt1* (CGI2300), ENSMUST00000065084.1, *Pdx1* and *Plcd3* showed lower levels in colon tumors than those in mock-treated normal colonic epithelial cells (Figure 5). These results suggested that some of the aberrant H3K27me3 induced in colonic epithelial cells was functionally involved in colon carcinogenesis.

Acquired H3K27me3 was followed by aberrant DNA methylation

A role of acquired H3K27me3 as a pre-mark for induction of aberrant DNA methylation was examined by analyzing DNA methylation levels of *Abca1*, *Dapk1*, *Gramd1b*, *Hdac5*, *Tbc1d16* and *Zfpm1* in FACS-purified colonic epithelial cells of mice 34 weeks after the initiation of DSS treatment. Among the six regions analyzed, *Dapk1* showed an increased DNA methylation level in colonic epithelial cells exposed to colitis (Figure 6). Two regions, *Hdac5* and *Tbc1d16*, showed high DNA methylation levels even in the mock-treated group, and methylation levels decreased by colitis. Three other regions, *Abca1*, *Gramd1b* and *Zfpm1*, were unmethylated in both groups. This result indicated that acquired H3K27me3 could function as a pre-mark for aberrant DNA methylation as pre-existing H3K27me3.

Discussion

In this study, we showed that aberrant H3K27me3 could be induced *in vivo* by exposure to a specific environment, here DSS-induced colitis, for the first time. The alterations of the H3K27me3 levels were probably involved in the formation of a field defect, and indicated to function as a pre-mark for induction of aberrant DNA methylation.

The involvement of the aberrant H3K27me3 in the field defect was indicated by the association between the altered H3K27me3 levels and altered gene expression, its persistence even after the disappearance of colitis and the presence of the alterations of H3K27me3 levels in colon tumors. If the alterations of the H3K27me3 levels are simple passengers, they are expected to be present in cancer tissues simply according to the frequency in non-cancer tissues. Nevertheless, such alterations were frequently present in tumors, and this indicated that the H3K27me3 alterations were functionally involved in carcinogenesis. Indeed, among the genes with increased H3K27me3 levels and frequently present in tumors, *Dapk1* is known as a positive mediator of apoptosis (31), and downregulated in various hematologic malignancies (32–34). Therefore, it is suggested that aberrant H3K27me3 induced by exposure to a specific inducer in normal-appearing tissues is involved in the formation of a field defect.

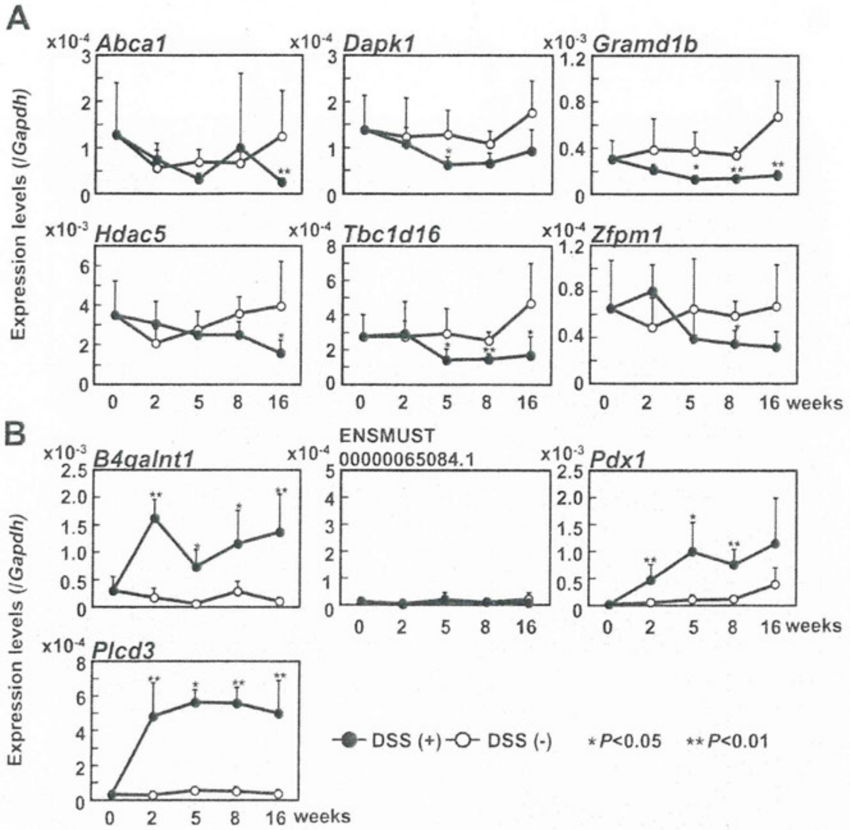

Fig. 4. Association between altered H3K27me3 levels and altered gene expression. (**A**) Temporal profiles of expression of genes with increased H3K27me3 levels. Gene expression was analyzed in colonic epithelial cells by qRT-PCR. *Dapk1*, *Gramd1b*, and *Tbc1d16* expression decreased at five weeks, but *Hdac5* and *Zfpm1* expression decreased at late phases of colitis. Black and white circles show DSS-treated ($n = 5$) and mock-treated ($n = 5$) groups, respectively. The significance of difference was evaluated by the Mann–Whitney *U*-test (*$P < 0.05$, **$P < 0.01$). (**B**) Temporal profiles of expression of genes with decreased H3K27me3 levels. *B4galnt1*, *Pdx1*, and *Plcd3* had increased expression at 2 weeks.

To prove the involvement of aberrant H3K27me3 in the formation of a field defect, intervention using specific inhibitors of histone H3K27 methyltransferase, Ezh2, and demethylases, Kdm6a and Kdm6b, is expected to provide important information. However, although 3-deazaneplanocin A (DZNep) is used for the inhibition of H3K27me3, it also affects other histone modifications such as H3K4me3 and H3K9me2 (35). Therefore, the precise role of aberrant H3K27me3 in the formation of a field defect cannot be assessed at this moment, and should be assessed once specific inhibitors of these enzymes are developed.

Acquired H3K27me3 at *Dapk1* also was indicated to function as a pre-mark for induction of aberrant DNA methylation. Although most of the methylated genes in cancer cells have H3K27me3 in normal cells (19–24,36), a small fraction of genes, including tumor-suppressor genes, are methylated in cancer cells despite the absence of H3K27me3 in normal cells (37). H3K27me3 levels of *Dapk1*, known as a tumor-suppressor gene, were increased by exposure to inflammation, and then aberrant DNA methylation was induced. Therefore, acquisition of a pre-mark, H3K27me3 by environmental exposure might be one of the mechanisms how aberrant DNA methylation is induced in tumor-suppressor genes that originally do not have the pre-mark, in addition to the mechanism of selection of rare events due to the growth advantage conferred (4).

Hdac5 showed a decrease in DNA methylation level despite its increase in the H3K27me3 level by DSS-induced colitis. Different from *Dapk1*, DNA methylation level was originally high at *Hdac5*. Generally, at regions whose DNA methylation level is originally high, H3K27me3 levels are increased after the removal of DNA methylation (38) due to the inhibitory effect of DNA methylation on the PRC2 recruitment (39). Therefore, it is possible that the decrease in DNA methylation level at *Hdac5* promoted the recruitment of PRC2, and led to the increase in the H3K27me3 levels.

As for the mechanisms of aberrant H3K27me3 induction, dysfunction of genes involved in the regulation of H3K27me3 can be considered. EZH2 is known to be upregulated in various human cancers including bladder, breast, gastric and prostate cancers, and these upregulations are known to be associated with poor prognosis (40–43). However, contrary to expectations, expression levels of genes involved in the regulation of H3K27me3 were not altered by exposure to DSS-induced colitis. Therefore, it is possible that localization or enzymatic activities of these factors are altered by exposure to DSS-induced colitis, and these alterations might be involved in aberrant H3K27me3 induction in colonic epithelial cells.

As for the mechanisms of persistence of aberrant H3K27me3 even after the disappearance of DSS-induced colitis, the maintenance mechanism of H3K27me3 by EZH2 (44,45) is probably involved. Namely, EZH2 at a replication site binds to H3K27me3 and introduces methyl groups to newly recruited histones. This maintenance mechanism in stem cells that can produce progenitor or differentiated cells seems to be involved in the persistence of aberrant H3K27me3 found here.

Alterations of other repressive histone modifications such as H3K9me2 and H3K9me3 were also induced in colonic epithelial cells by exposure to DSS-induced colitis, and regions with those alterations hardly overlapped with regions with H3K27me3-level alterations. Therefore, alterations of these repressive histone modifications

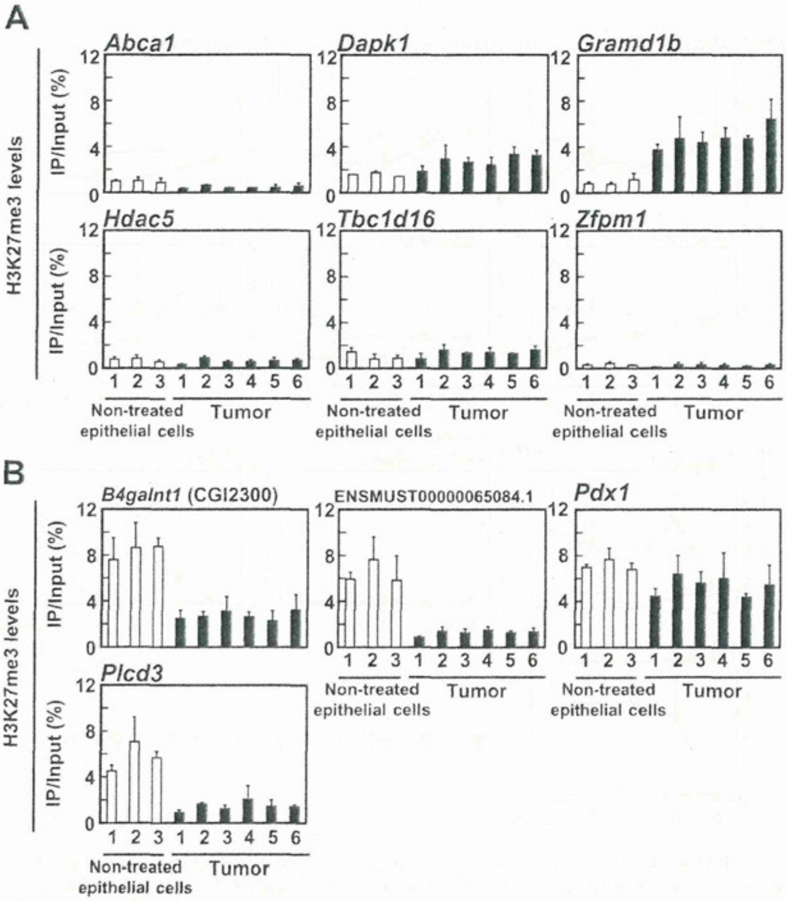

Fig. 5. H3K27me3 levels in colon tumors and age-matched normal colonic epithelial cells (non-treated). *Dapk1* and *Gramd1b* frequently showed high H3K27me3 levels in colon tumors (**A**), and *B4galnt1* (CGI2300), ENSMUST00000065084.1, *Pdx1* and *Plcd3* frequently showed low H3K27me3 levels in colon tumors (**B**). The frequent carryover of the altered H3K27me3 levels into tumors suggested that these alterations were functionally involved in tumor development. Error bars represent the experimental errors.

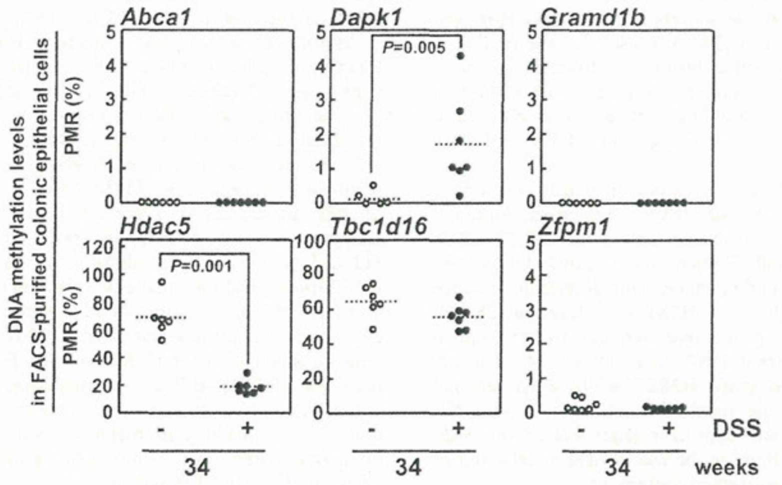

Fig. 6. DNA methylation analysis of genes with acquired H3K27me3. DNA methylation levels were analyzed by quantitative methylation-specific PCR in FACS-purified colonic epithelial cells. *Dapk1* showed increased DNA methylation levels in the DSS-treated group, indicating acquired H3K27me3 functioned as a pre-mark of DNA methylation induction. Black and white circles show DSS-treated ($n = 7$) and mock-treated ($n = 6$) groups, respectively. The significance of difference was evaluated by the Mann–Whitney *U*-test. Note that scales of the longitudinal axes are different for *Hdac5* and *Tbc1d16* from the others. PMR, the percentage of methylation reference.